



CENTRE DE RECERCA MATEMÀTICA

Title: *Power Law Size Distributions in Geoscience Revisited*
Journal Information: *Earth and Space Science*
Author(s): Álvaro Corral and Álvaro González.
Volume, pages: 673-697, DOI:[www.doi.org/10.1029/2018ea000479]



REVIEW ARTICLE

10.1029/2018EA000479

Special Section:

Nonlinear Systems in Geophysics:
Past Accomplishments and Future
Challenges

Key Points:

- We reanalyze the size distribution of earthquakes, karst sinkholes, wildfires, tropical cyclones, rainfall clusters, and impact fireballs
- A same, objective, statistical fitting method is improved and applied, allowing faithful comparisons between data sets
- The method automatically identifies the truncations of power law distributions, crossovers between power law regimes, and the best fit in the comparison between power law and lognormal tails

Correspondence to:

Á. Corral,
alvaro.corral@uab.es

Citation:

Corral, Á., González, Á. (2019). Power law size distributions in geoscience revisited. *Earth and Space Science*, 6, 673–697. <https://doi.org/10.1029/2018ea000479>

Received 20 SEP 2018

Accepted 12 APR 2019



Accepted article online 29 APR 2019

Published online 31 MAY 2019

©2019. The Authors.

This is an open access article under the terms of the Creative Commons Attribution-NonCommercial-NoDerivs License, which permits use and distribution in any medium, provided the original work is properly cited, the use is non-commercial and no modifications or adaptations are made.

Power Law Size Distributions in Geoscience Revisited

Álvaro Corral^{1,2,3,4}  and Álvaro González¹ 

¹Centre de Recerca Matemàtica, Edifici C, Campus Bellaterra, Barcelona, Spain, ²Departament de Matemàtiques, Universitat Autònoma de Barcelona, Barcelona, Spain, ³Barcelona Graduate School of Mathematics, Edifici C, Campus Bellaterra, Barcelona, Spain, ⁴Complexity Science Hub Vienna, Vienna, Austria

Abstract The size or energy of diverse structures or phenomena in geoscience appears to follow power law distributions. A rigorous statistical analysis of such observations is tricky, though. Observables can span several orders of magnitude, but the range for which the power law may be valid is typically truncated, usually because the smallest events are too tiny to be detected and the largest ones are limited by the system size. We revisit several examples of proposed power law distributions dealing with potentially damaging natural phenomena. Adequate fits of the distributions of sizes are especially important in these cases, given that they may be used to assess long-term hazard. After reviewing the theoretical background for power law distributions, we improve an objective statistical fitting method and apply it to diverse data sets. The method is described in full detail, and it is easy to implement. Our analysis elucidates the range of validity of the power law fit and the corresponding exponent and whether a power law tail is improved by a truncated lognormal. We confirm that impact fireballs and Californian earthquakes show untruncated power law behavior, whereas global earthquakes follow a double power law. Rain precipitation over space and time and tropical cyclones show a truncated power law regime. Karst sinkholes and wildfires, in contrast, are better described by truncated lognormals, although wildfires also may show power law regimes. Our conclusions only apply to the analyzed data sets but show the potential of applying this robust statistical technique in the future.

1. Introduction

Power law distributions, or more correctly, power law-like probability distributions, first appeared in the study of the natural world in relation with some “human affairs.” It seems that the pioneer work was that of Vilfredo Pareto, who, at the end of the nineteenth century, reported one of such distributions accounting for the wealth of individuals (Kagan, 2014; Pareto, 1897). Some years later, Auerbach and Estoup showed that the population of cities and the frequency of words in texts, respectively, follow essentially the same statistical pattern (Newman, 2005). Since then, many social (Axtell, 2001; Clauset et al., 2009), technological (Adamic & Huberman, 2002), communication (Corral et al., 2015; Moreno-Sánchez et al., 2016; Serrà et al., 2012), and biological systems (Camacho & Solé, 2001; Furusawa & Kaneko, 2003; Pueyo & Jovani, 2006) have been found to display what is now called Zipf’s law (Li, 2002), a type of power law-like distribution that appears when counting the number of entities that constitute collections of entities, with the remarkable characteristic that the power law exponent takes values close to 2. In geoscience, considerable interest in power law distributions appeared in the 1980s of the past century. It was the appealing work of Mandelbrot on fractals (Mandelbrot, 1983) which drew attention to the distribution of sizes of diverse geological objects and structures, like lakes, faults, fault gouge, oil reservoirs, sedimentary layers, and even asteroids (Turcotte, 1997). Nevertheless, some of these systems had been explored much earlier; for instance, Bennet studied fragments of broken coal in 1936, Korcak dealt with the distribution of islands in 1940, and the distribution of lunar craters was reported in the 1930s separately by McDonald and Young (Cross, 1966). Turcotte (1997) provides valuable bibliography on these issues. Remarkably, for these systems, when size is measured in terms of a linear dimension (e.g., diameter), the power law exponents are considerably larger than 2; they typically range from 2.4 to more than 4.

Around 1990, after the illuminating theory of Bak and coworkers on self-organized critical phenomena (Bak, 1996; Watkins et al., 2016), the interest in power law distributions was reinforced, in particular regarding the “severity” or “size” of natural disasters and other catastrophic geophysical phenomena that can be considered to happen in terms of “avalanches” (events which suddenly release energy slowly accumulated in the

system over a period). But it was 60 years earlier (1932) that Wadati had assumed a power law distribution for the energy of earthquakes, whereas Ishimoto and Iida published in 1939 a power law for the distribution of earthquake amplitudes recorded by a microseismograph (Utsu, 1999). Nowadays, these two power laws are known to be different representations of the Gutenberg-Richter law of earthquake size (Kagan, 2002; Kanamori & Brodsky, 2004). Following the seminal work of Bak (Bak, 1996; Bak et al., 1987), many authors claimed power law distributions in systems as diverse as volcanic eruptions, rockfalls, landslides, forest fires, solar flares, pulsar glitches, or biological extinctions (Bak, 1996; Malamud, 2004). Again, in contrast to Zipf's law, the power law exponent is not constrained to be around 2 but shows considerable scatter between 1 and 2, depending on the system under consideration.

An important drawback of these studies has been statistical rigor. In most cases, the evidence for power law distributions was just an apparent linear behavior in a log-log representation of the probability density or of the complementary cumulative distribution. In some other cases, a linear regression straight line was fit by the least squares method, a procedure which can lead to substantial biases and wrong inferences when applied to probability distributions (Clauset et al., 2009; White et al., 2008). More recent works have made an effort to improve the statistical methodology.

In this paper, we attempt to give an overview of power law distributions in geoscience; however, due to the heterogeneity of the approaches, a proper and fair comparison of results is impossible, and we have opted for a revision of paradigmatic systems using a rigorous statistical protocol, which is an improvement of a previous one (Deluca & Corral, 2013). Although the definitive recipe to fit power law distributions does not yet exist, the method developed here is reasonable enough and fully objective. Due to many limitations, our overview of power laws is far from systematic and we have selected instead a few representative examples across the geosciences.

We will concentrate on the (spatial) size of structures on the solid Earth and atmosphere (karst sinkholes and rain clusters) and on the size, in terms of energy or severity, of diverse natural events (earthquakes, wildfires, tropical cyclones, amount of rainfall, and impact fireballs). All these examples relate to potentially damaging natural phenomena for which adequate fits of their size distribution are especially important, given that these fits (together with the temporal occurrence rate) are used for assessing the long-term hazard these phenomena pose. Further examples with potential power law distributions have been quoted in geology (Burroughs & Tebbens, 2001; Turcotte, 1997), hydrology (Aban et al., 2006), ecology (White et al., 2008), and astrophysics (Aschwanden, 2013). We will not be able to approach other interesting geophysical variables, such as distances between events and jumps (Corral, 2006; Davidsen & Paczuski, 2005; Felzer & Brodsky, 2006) or such as durations and waiting times (Corral, 2015), which have also been related in some way to power law distributions, for example, for earthquakes (Bak et al., 2002; Corral, 2004), volcanic eruptions (Cannavò & Nunnari, 2016), solar flares (Baiesi et al., 2006; Boffetta et al., 1999), solar wind (Wanliss & Weygand, 2007), or geomagnetic storms (Moriña et al., 2019). Possible power law distributions of so-called intensive variables, such as rain rate (Peters et al., 2010; Yano et al., 2004), are also disregarded in this paper.

As mentioned in the first paragraphs, power law-like distributions are far from being exclusive of geoscience (Li, 2002). The interested reader can find extensive bibliography for biological systems (Muñoz, 2018), neuroscience (Chialvo, 2010), economy (Farmer & Geanakoplos, 2008), and technology (Adamic & Huberman, 2002). The ubiquity of power law-like distributions has induced some authors to claim for a common origin for them (Bak et al., 1987; Bak, 1996), although a large variety of alternative explanations has been proposed (Corominas-Murtra et al., 2015; Ferrer-i-Cancho, 2016; Miller, 1957; Mitzenmacher, 2004; Newman, 2005; Penland & Sardeshmukh, 2012; Saichev et al., 2009; Simkin & Roychowdhury, 2011; Simon, 1955; Sornette, 2004; Tria et al., 2014). Our statistical analysis will not allow us to enter into mechanistic and generative models and the debate associated to them; nevertheless, in the last section we provide a summary of these explanations.

Thus, in the next section we explain untruncated and truncated power law distributions and the nuances that distinguish them from power law-like distributions. Then, we expose our procedure to fit power law-like distributions (which also applies to the lognormal and could be immediately extended to any other distribution). We also explain a likelihood-ratio test to distinguish between power law tails and lognormal tails. Finally, section 4 explains the data sets analyzed as well as the results obtained from them. The conclusions are at the end.

2. Power Law Distributions and Power Law-Like Distributions

Let us recall that the probability density $f(x)$ of a continuous random variable is defined as the probability that the random variable is between the values x and $x + dx$, divided by dx , where dx is the width of the interval (also called bin). In the ideal mathematical case dx goes to zero (Ross, 2010) but in practice dx has to be wide enough to make it possible the counting of several events per interval. In geoscience x may represent the size of some geological structure (faults, islands, lakes, etc.) or of some geophysical phenomenon (energy of earthquakes, amount of rain, etc.). It is noteworthy that $f(x)$ is not a probability but a density of probability, so it is a physical quantity with units of x^{-1} .

Equivalently, the probability distribution can be described in terms of the complementary cumulative distribution function, $S(x)$, which provides the probability that the random variable takes a value above x . Both functions are related by means of

$$f(x) = -\frac{dS(x)}{dx} \quad \text{and} \quad S(x) = \int_x^{\infty} f(x')dx'$$

Note that $f(x)$ fulfills $f(x) \geq 0$ and $\int_{-\infty}^{\infty} f(x)dx = 1$ (normalization), whereas $S(x)$ is a nonincreasing function of x with $\lim_{x \rightarrow -\infty} S(x) = 1$ (normalization) and $\lim_{x \rightarrow \infty} S(x) = 0$. In some literature it is difficult to guess if the authors are dealing with $f(x)$ or $S(x)$ or with some variation of any of them. Sometimes, when $f(x)$ or $S(x)$ are estimated from data, their dependence on x is referred to as the frequency-size relationship or even the size-frequency distribution.

2.1. Untruncated Power Law Distribution

A continuous variable x is power law (pl) distributed (Johnson et al., 1994) if its probability density is given by

$$f_{\text{pl}}(x) = \frac{C}{x^{\beta}}$$

for $x \geq a$ and $f_{\text{pl}}(x) = 0$ for $x < a$, with $\beta > 1$ and a the lower cutoff or lower truncation, fulfilling $a > 0$. Normalization implies that the normalization constant C is determined by a and β , and so

$$f_{\text{pl}}(x) = \frac{\beta - 1}{a} \left(\frac{a}{x}\right)^{\beta} \quad (1)$$

for $x \geq a$.

In terms of the complementary cumulative distribution the power law is defined as

$$S_{\text{pl}}(x) = \left(\frac{a}{x}\right)^{\beta-1} \quad (2)$$

for $x \geq a$ and $S_{\text{pl}}(x) = 1$ for $x < a$. Note that there is some ambiguity regarding the power law exponent, which is β for $f_{\text{pl}}(x)$ and $\beta - 1$ for $S_{\text{pl}}(x)$. We take the convention that the exponent of the distribution is β , the exponent of the density. In order to distinguish the power law distribution from the (upper) truncated power law, introduced below, sometimes we may talk about “untruncated power law,” referring to the former, although both distributions are unavoidably truncated from below ($a > 0$).

Two important properties of power law distributions are scale invariance and divergence of moments. The first one means that power laws remain the same after appropriate changes of scale in x and $f(x)$; for instance, if $f(x) \propto 1/x^{3/2}$, the change $x \rightarrow 100x$ and $f \rightarrow f/1000$ leaves the resulting function the same (this does not happen with an exponential, e.g., nor with any other function different than the power law). Thus, scale invariance implies that no characteristic scale exists (Christensen & Moloney, 2005; Corral, 2008; Takayasu, 1989). Nevertheless, strictly speaking, scale invariance holds for power laws defined in the whole range $x > 0$ (e.g., Newton’s law of gravitation), whereas due to normalization, power law distributions are defined for $x \geq a > 0$; this prevents true scale invariance; in other words, the value of a sets a characteristic scale, so one only may talk of scale invariance above the lower cutoff a .

Interestingly, for some systems the cutoff a seems to be so small that its value is unknown, which implies that no characteristic scale shows up. This is the case of earthquakes, for instance. So the question “which is the typical size of earthquakes in Japan or California?” cannot be answered, as no characteristic size can be defined. Due to their scale-invariant properties, power law distributions are sometimes called fractal

distributions, as by Turcotte (1997); nevertheless, we prefer the former terminology, which does not contain any implicit reminiscence of self-similar geometry (one can ignore spatial structure, if it exists).

Divergence of moments means that if, for instance, the exponent is $\beta \leq 2$, the mean or expected value of the variable (the first moment), $\langle x \rangle = \int_{-\infty}^{\infty} x f(x) dx$, becomes infinite, in the same way that all higher moments, $\langle x^k \rangle = \int_{-\infty}^{\infty} x^k f(x) dx$, with $k \geq 1$. If $2 < \beta \leq 3$, the first moment is finite but the second moment $\langle x^2 \rangle$ and higher moments become infinite, and so on. Divergence of moments has the annoying consequence that some important results of probability theory do not hold, as the law of large numbers when $\beta \leq 2$ (Corral, 2015; Shiryayev, 1996). So, in this case one cannot estimate the mean of the distribution from the sample mean, simply because the mean of the distribution is infinite and the sample mean cannot converge to this value (Corral & Font-Clos, 2013). If $2 < \beta \leq 3$, the standard central limit theorem does not apply and the sample mean neither follows Gaussian statistics nor has a finite variability (Bouchaud & Georges, 1990). If one takes logarithms on the expressions of $f_{pl}(x)$ or $S_{pl}(x)$ for a power law distribution, one immediately realizes that both $\ln f_{pl}(x)$ and $\ln S_{pl}(x)$ are linear functions of $\ln x$. If the least squares method is applied to the logarithm of the empirical estimations of $f(x)$ or $S(x)$, one can get an estimation of the parameters β and a . However, one cannot do inference with the resulting parameters, as some requirements of the theory of linear regression are not fulfilled. In addition, obtaining an accurate empirical estimation of $f(x)$ is not straightforward, as one needs to choose bins in a proper way (Deluca & Corral, 2013; Wand, 1997). Let us clarify that the least squares method is inappropriate to estimate probability distributions but not to establish linear correlation between two variables, x and y (or $\log x$ and $\log y$), for instance, nor to curve fitting in general.

Despite the peculiar properties of power law distributions, estimation of their parameters is straightforward using maximum likelihood. This is a method of estimation of parameters that gathers a number of desirable properties (Casella & Berger, 2002), such as invariance under reparameterization (the resulting estimated distribution does not depend on the choice of parameters) and invariance under change of variables (the resulting description of the phenomenon does not depend on the selected random variable). When applied to probability distributions that belong to the so-called exponential family (both power laws and truncated power laws belong to this family, as well as the lognormal, truncated or not), maximum likelihood estimators turn out to fulfill consistency (they are unbiased and convergent, asymptotically; i.e., the estimation tends to the true value if the number of data is large), due to the uniqueness of the maximum (Pawitan, 2001), and also fulfill asymptotic efficiency (they achieve the Cramér-Rao lower bound asymptotically, i.e., the estimation tends to have the smallest possible variance among all the unbiased estimators) under some standard regularity conditions (Pawitan, 2001).

The maximum likelihood estimation of the power law exponent yields (Clauset et al., 2009; Deluca & Corral, 2013)

$$\beta_{pl} = 1 + \frac{1}{\ln(g/a)}, \quad (3)$$

where g is the geometric mean of the sample, defined as $\ln g = n^{-1} \sum_{i=1}^n \ln x_i$, with n the size of the sample and x_i the n observations of the random variable. As β is determined from the sample, it is subject to statistical uncertainty (it is a “statistic”) and its standard deviation or standard error is

$$\sigma_{\beta} = \frac{\beta - 1}{\sqrt{n}}, \quad (4)$$

where β has to be understood here as the true value of the exponent (not the estimated one, although they will be very close if n is large). Regarding the cutoff a , it is estimated as $a_{pl} = \min(x_1, \dots, x_n)$. The reason is that as long as $x_i \geq a$ for all i , the larger a , the higher the likelihood. However, if a single i fulfills $x_i < a$, then the likelihood becomes zero (as $f_{pl}(x_i) = 0$). This implies that a has to grow up to the smallest value of x_i but not more.

Which is then the problem with power laws, if this estimation procedure is so straightforward? The key issue is that in practice one does not deal with (pure) power law distributions but with power law-like distributions. These constitute a loose family of distributions (Farmer & Geanakoplos, 2008) with the characteristic that, for a certain range of x , the distribution resembles in some undefined way a power law. Consider the

so-called full-tails gamma (ftg) distribution (del Castillo et al., 2017)

$$f_{\text{ftg}}(x) = \frac{1}{\theta_2 \Gamma(1 - \beta, \theta_1/\theta_2)} \left(\frac{\theta_2}{\theta_1 + x} \right)^\beta \exp\left(-\frac{\theta_1 + x}{\theta_2}\right),$$

with $\theta_1 > 0$, $\theta_2 > 0$, and $-\infty < \beta < \infty$ and with $\Gamma(1 - \beta, \theta_1/\theta_2)$ the (upper) incomplete gamma function (Abramowitz & Stegun, 1965). This distribution is a truncated gamma distribution (Serra & Corral, 2017) extended to $1 - \beta < 0$ and shifted to have support in the interval $[0, \infty)$. Let us consider $\theta_1 \ll \theta_2$. In this case the distribution resembles a power law in some range $a \leq x \leq b$, with $\theta_1 \ll a$ and $b \ll \theta_2$, but, strictly speaking, that part of the distribution is not a power law. Interestingly, recent work (Voitalov et al., 2018) has identified power law-like distributions with regularly varying distributions, for which $S(x)$ is a power law multiplied by a slowly varying (unknown) function. This leads to asymptotic power laws, which is a concept in some cases similar but certainly different to our power law-like behavior (for which b can be finite).

In practice, the disadvantage is that the real underlying theoretical distribution $f(x)$ is unknown. For instance, simple branching processes (bp; which are mean field models by construction) yield discrete probability distributions for their total number of elements x , which (close to their critical point and for large x) lead to truncated gamma tails, $f_{\text{bp}}(x) \propto x^{-3/2} e^{-x/\theta}$ (Corral & Font-Clos, 2013); but branching processes with finite-size effects lead to more complicated functional forms for the tail, even in the critical case (Corral et al., 2018). Beyond mean field, little is known, and of course, real systems are more complicated than any model. On the other side, incompleteness effects for small values of x may provoke an underestimation on the count of x and a deviation from a power law behavior, as modeled, for instance, by the full-tails gamma distribution above or by the genuine Pareto (par) distribution $f_{\text{par}}(x) = (\beta - 1)\theta^\beta / (\theta + x)^\beta$; nevertheless, this sort of modeling is ad hoc.

In summary, there are a number of processes and factors that trigger deviations from power law behavior both for small and large values of x ; however, these factors are difficult to parameterize. If one can disregard large $-x$ deviations (perhaps because the number of data is so low that the scale of deviations is not sampled), one can model the data by a (pure) untruncated power law distribution, equations (1) and (2), but the meaning of the parameter a is totally different than in the original definition, as a defines the scale at which the small $-x$ deviations become negligible, and values of x below a need to be disregarded. The rest of values of x , those above a , will be considered in this paper to define the tail of the distribution. The main problem in fitting power law-like distributions is finding the lower cutoff a . Note that in this context we will need to distinguish between the total number of data N and the number of data in the power law range, n .

2.2. Truncated Power Law Distribution

If, in addition, there are deviations from power law behavior for large values of x and there is no information on the shape of the tail, the situation gets worse. An option is to fit a truncated power law (tpl) distribution (Aban et al., 2006; Burroughs & Tebbens, 2001; Deluca & Corral, 2013; Johnson et al., 1994) given by

$$f_{\text{tpl}}(x) = \frac{\beta - 1}{a(1 - c^{\beta-1})} \left(\frac{a}{x} \right)^\beta$$

for $a \leq x \leq b$ and $f_{\text{tpl}}(x) = 0$ otherwise, with $a > 0$, $b > 0$, $c = a/b$, and $-\infty < \beta < \infty$ (nevertheless, the case of negative exponent corresponds to an increasing power law and is of little interest; the case $\beta < 1$ allows $a \geq 0$). The limiting case $\beta = 1$ needs a separate formulation (Deluca & Corral, 2013). It has to become clear that we apply this distribution to the central part of the data, disregarding values of x outside the interval $[a, b]$. Of course, the major problem is to find appropriate values of a and b . Again, we will distinguish between the total number of data N and the number of data in the power law range, $a \leq x \leq b$, denoted as n .

The alternative description in terms of the complementary cumulative distribution yields

$$S_{\text{tpl}}(x) = \frac{(a/x)^{\beta-1} - c^{\beta-1}}{1 - c^{\beta-1}}$$

for $a \leq x \leq b$; $S_{\text{tpl}}(x) = 1$ for $x < a$ and $S_{\text{tpl}}(x) = 0$ for $x > b$. The limit $b \rightarrow \infty$ when $\beta > 1$ returns to the usual power law, equations (1) and (2). Note that for the truncated power law, $\ln f_{\text{tpl}}(x)$ is still a linear function of $\ln x$ but $\ln S_{\text{tpl}}(x)$ is not. When $\beta > 1$, linearity between $\ln S_{\text{tpl}}(x)$ and $\ln x$ only takes place for $x \ll b$.

The maximum likelihood estimation of the exponent β cannot be solved explicitly, and one is faced to the numerical maximization of the likelihood or, equivalently, of the per-datum log likelihood (Deluca & Corral, 2013)

$$\mathcal{L}_{\text{tpl}}(\beta) = \ln \frac{\beta - 1}{1 - c^{\beta-1}} - \beta \ln \frac{g}{a} - \ln a. \quad (5)$$

Care with numerical overflows must be taken when β gets close to one; see Deluca and Corral (2013). An analytical expression for the standard deviation of β can be derived (Aban et al., 2006; Deluca & Corral, 2013); nevertheless, we will not use it (the reasons will become clear later, section 3.2). In the same way, the maximum likelihood estimators of a and b , which are $a_{\text{tpl}} = \min\{x_1, \dots, x_n\}$ and $b_{\text{tpl}} = \max\{x_1, \dots, x_n\}$, will be meaningless for us, as these estimations assume that the data set is fixed, but we need to find precisely which subset of the data may follow a (truncated) power law.

2.3. Double Power Law Distribution

It may happen that some data set is well fit by a truncated power law from $x = a$ up to some value $x = b$, and from $x > b$ the data are also well fit by an untruncated power law. Let us relabel this crossover point as $b = \theta$. Then, it is clear that the data are fit by two power law regimes for $x > a$, and we may define the double power law (dpl) distribution as

$$f_{\text{dpl}}(x) = (1 - q) \frac{\beta_1 - 1}{\theta} \frac{1}{c^{1-\beta_1} - 1} \left(\frac{\theta}{x}\right)^{\beta_1} \quad \text{for } a \leq x \leq \theta,$$

$$f_{\text{dpl}}(x) = q \frac{\beta_2 - 1}{\theta} \left(\frac{\theta}{x}\right)^{\beta_2} \quad \text{for } \theta \leq x,$$

and zero for $x < a$ and where the parameter q is chosen to ensure continuity between the two regimes at $x = \theta$, leading to

$$q = \frac{\beta_1 - 1}{(\beta_2 - 1)c^{1-\beta_1} - (\beta_2 - \beta_1)}$$

and the two exponents fulfilling $-\infty < \beta_1 < \infty$ and $\beta_2 > 1$, $c = a/\theta$ and with $a > 0$ if $\beta_1 > 1$ and $a \geq 0$ if $\beta_1 < 1$. The complementary cumulative distribution function leads to

$$S_{\text{dpl}}(x) = q + (1 - q) \frac{(\theta/x)^{\beta_1-1} - 1}{c^{1-\beta_1} - 1} \quad \text{for } a \leq x \leq \theta,$$

$$S_{\text{dpl}}(x) = q \left(\frac{\theta}{x}\right)^{\beta_2-1} \quad \text{for } \theta \leq x,$$

and zero for $x < a$. The sudden change of slope at $x = \theta$ is unlikely to fit real-world distributions with a large number of data, so some refinement in the parameterization may be needed to fit properly the crossover in this case.

2.4. Change of Variables

A noteworthy issue comes from the fact that the variable x is not uniquely defined. For example, in terms of size of objects, x can be the linear size, denoted by L or can be the volume V . Assuming a general relation between both, $V \propto L^z$ (with $z = 3$ for spherical or cubic objects), it can be shown that if one of them is power law distributed, so is the other, both for untruncated and for truncated power laws (and also for the double power law), and the power law exponents are related by

$$z = \frac{\beta_L - 1}{\beta_V - 1}. \quad (6)$$

This relation explains, at least in part, why the exponents β_L of the distributions of geological objects become so large (even larger than 4) when the size is defined in terms of the linear size L . In terms of the volume V the exponents become smaller. Note that this simple relation does not apply to the more complicated scenario that arises, for example, when volumes have to be calculated from random cross sections (Gaonac'h et al., 1996); see also Baddeley and Vedel Jensen (2005).

3. Fitting of Power Law-Like Distributions

3.1. Clauset et al.'s Procedure

Drawbacks in fitting power law distributions were pointed out by Clauset et al. (2009) but were previously noticed by other authors, such as Goldstein et al. (2004), Bauke (2007), and White et al. (2008). There is an important confusion regarding the method and achievements of Clauset et al. (2009), as many authors claim that they are using this method while they are just fitting by plain maximum likelihood estimation. Summarizing, the Clauset et al.'s method (for an untruncated power law distribution) proceeds in two parts. For the first part one calculates a tentative fit as follows

1. Pick a value of the lower cutoff a .
2. Fit, by maximum likelihood, a power law to the range $x \geq a$ (using equation (3)). A value of β is obtained.
3. Calculate the Kolmogorov-Smirnov distance between the empirical distribution (for $x \geq a$) and the theoretical distribution (using the value of β obtained in the previous step).

Repeat the procedure for all possible values of the lower cutoff and select the one which yields the minimum Kolmogorov-Smirnov distance. The selected value of a has an associated value of the exponent β , and both parameters define the tentative fit.

The second part of the procedure assigns a p value to the fit. One only needs to generate samples with the same number of data than the original empirical data. These samples are obtained from bootstrap of the empirical data for $x < a$ and are simulated synthetic power laws for $x \geq a$ (with the resulting value of β). Applying the first part of the procedure to any of the synthetic samples, one obtains a distribution of the minimized Kolmogorov-Smirnov distance, which allows one to define a p value as the probability that the minimized distance takes a value larger than the one obtained empirically. At the end, the recipe is: Reject the tentative fit if the p value is too low, according to the desired significance level; otherwise, there is no reason for rejection and the power law fit is “accepted.”

Unfortunately, we have encountered several drawbacks of the Clauset et al.'s method. First, the method is ad hoc and there is no justification why the minimization of the Kolmogorov-Smirnov distance should work to find a meaningful value of a (Deluca & Corral, 2013). Second, the method cannot be extended to truncated power law distributions (i.e., it is only prescribed for $b \rightarrow \infty$). And third, we have found the method to fail when applied to simulated data with real power law tails, since the power law is rejected, despite it is a real, synthetic power law (Corral et al., 2011). Other authors have criticized also Clauset et al.'s method (Voitalov et al., 2018). In general, power law fitting is a controversial issue (Barabási, 2018; Holme, 2019). Therefore, despite the popularity of the Clauset et al.'s method, we have developed an alternative procedure.

3.2. Alternative Power Law Fitting Procedure

Our method is close somehow to the one of Clauset et al., in the sense that it is based on both maximum likelihood estimation (Pawitan, 2001) and on the Kolmogorov-Smirnov goodness of fit test (Press et al., 1992). The version presented here is a straightforward extension of a previous work (Deluca & Corral, 2013; Peters et al., 2010). We explain the case of truncated power laws; simplification to untruncated power laws is trivial:

1. Pick a value of the lower cutoff a and another value of the upper cutoff b .
2. Fit, by maximum likelihood, a truncated power law to the range $a \leq x \leq b$ (maximizing equation (5)). A value of β is obtained.
3. Calculate the Kolmogorov-Smirnov distance between the empirical distribution (restricted to $a \leq x \leq b$) and the theoretical distribution (using the value of β obtained above).
4. Assign a p value to the resulting tentative fit, in the following way:
 - Simulate a synthetic power law in the range $a \leq x \leq b$, with the value of β just obtained, and with the same number of data n .
 - Apply to the synthetic data the previous two steps (fit of β and calculation of Kolmogorov-Smirnov distance with the new value of β).

Repeat the simulation procedure many times in order to obtain the distribution of the Kolmogorov-Smirnov distance (the theoretical distribution cannot be used because β is calculated from the same data to which we apply the test). The p value is obtained as the probability that this distance is larger than the empirical distance.

Repeat this procedure for all possible values of a and b . If more than one pair of values yield “acceptable” p values (higher than the significance level p_{\min}), choose the pair of a and b that leads to the largest ratio b/a (this is the largest power law log-range), and the resulting values of a , b , and β give the resulting “accepted” fit. If no high enough p values are found, the power law is rejected. In this paper we take a demanding significance level $p_{\min} = 0.20$. Note that this applies to continuous random variables, while the fitting of discrete power laws is a bit more involving (Corral et al., 2012).

This is the original procedure (Deluca & Corral, 2013; Peters et al., 2010), which has an important drawback: it does not allow to estimate the uncertainty of the cutoffs a and b . Moreover, the uncertainty in the exponent β was obtained from the standard deviation of the maximum likelihood estimation, equation (4) or the equivalent one for the truncated case (Aban et al., 2006), which assumed a and b fixed. Therefore, we expect the real uncertainty in β to be larger.

This problem, or these two related problems, is solved here in a very simple way. We just take bootstrap resamplings of the original data (Good, 2011) and repeat the whole procedure with them; this will allow to obtain distributions for a , b , and β , from which their uncertainty can be estimated. This method will be applied to diverse geophysical data in the next sections. Moreover, as the distributions of both cutoffs are somewhat asymmetric, we consider their logarithms (which are more symmetric) and report the uncertainty of the cutoffs using one standard deviation of the logarithms. Bootstrap was used in a similar context by Woessner and Wiemer (2005), in order to estimate the uncertainty of the magnitude of completeness of seismic catalogs. Note that although it has been recognized that bootstrap can lead to biased information when dealing with extreme value distributions, our estimation procedure does not make use of those distributions; in fact, the only statistic that is involved in the estimation is a mean value (that of the logarithm of the random variable, equations (3) and (5)).

The method can be complemented by studying the dependence of the exponent β on both cutoffs (Baró & Vives, 2012), taking cutoff values inside the power law range found (a , b). In a real power law, β should be stable against increases in a and decreases in b ; conversely, a trend of β as a function of a or b is an indication of a spurious power law (it may happen when the number of data is low, as then rejection of the power law gets more difficult). Interestingly, the resulting dependence on the cutoffs could be used to identify an alternative distribution to the power law, if the resulting exponent does not show a flat behavior (Salje et al., 2017).

For the fitting of an untruncated power law distribution we introduce an additional improvement. We impose that the range of variation of the lower cutoff a does not cover the whole range of x but only the range $a > a_{cv}$ for which an untruncated power law can be considered to be a better fit than a truncated lognormal. This is developed in the next subsection.

3.3. Comparison of Untruncated Power Law Versus Truncated Lognormal

In addition to evaluate if a power law distribution is a good fit in some range of a particular data set, one may compare the power law in front of diverse alternative distributions (Clauset et al., 2009). Particularly important and widely used in the same context (Corral et al., 2008; Hantson et al., 2016; Malevergne et al., 2011; Turcotte, 1997) is the lognormal case (Johnson et al., 1994; Limpert et al., 2001) for which a likelihood-ratio test can be applied in a very simple way, comparing the untruncated power law with the truncated lognormal (the term truncated here refers to a lower truncation of the lognormal; the power law is always lower truncated, due to normalization). In the most general case, the truncated lognormal (tln) distribution is defined by the probability density

$$f_{\text{tln}}(x) = \sqrt{\frac{2}{\pi}} \left[\operatorname{erfc} \left(\frac{\ln a - \mu}{\sqrt{2}\sigma} \right) - \operatorname{erfc} \left(\frac{\ln b - \mu}{\sqrt{2}\sigma} \right) \right]^{-1} \frac{1}{\sigma x} \exp \left(-\frac{(\ln x - \mu)^2}{2\sigma^2} \right)$$

for $a \leq x \leq b$ (and zero otherwise), with $-\infty < \mu < \infty$, σ positive, the cutoffs a and b also positive, and $\operatorname{erfc}(y) = \frac{2}{\sqrt{\pi}} \int_y^\infty e^{-x^2} dx$ the complementary error function (unfortunately, with this parameterization μ and σ have no clear physical meaning). Except in one particular case, we consider b^{-1} fixed to 0, for which the second erfc term goes to zero. This distribution will be sometimes simply referred here as lognormal, for economy of language. The true (untruncated) lognormal distribution is recovered in the limit $a \rightarrow 0$ and $b \rightarrow \infty$. Note that in contrast to other fitting methods, where the normalization constant can be an additional parameter, both maximum likelihood estimation and the Kolmogorov-Smirnov test require the

exact computation of the normalization constant (this is the reason of the apparent complication of the expression for $f_{\text{lin}}(x)$).

The comparison procedure is based in the calculation of the residual coefficient of variation cv_{ℓ} of the logarithm of the rescaled random variable (Malevergne et al., 2011). We need to define $x_{(i)}$ as the i th value of the variable when this is sorted in an increasing way, that is, $x_{(1)} \leq x_{(2)} \leq \dots \leq x_{(N)}$. Then,

$$cv_{\ell} = \frac{s_{\ell}}{m_{\ell}},$$

with m_{ℓ} the mean of the new variable ℓ defined as the logarithm of the variable rescaled by $x_{(k)}$, that is, $\ell = \log(x/x_{(k)})$, which is calculated for the $n = N - k$ values of the original variable fulfilling $x > x_{(k)}$ (we assume the variable x is continuous and disregard the case in which some value of x is repeated in the data set), so

$$m_{\ell} = \frac{1}{n} \sum_{i=k+1}^N \log \frac{x_{(i)}}{x_{(k)}}.$$

In addition, s_{ℓ}^2 is the unbiased variance of ℓ , that is,

$$s_{\ell}^2 = \frac{1}{n-1} \sum_{i=k+1}^N \left(\log \frac{x_{(i)}}{x_{(k)}} - m_{\ell} \right)^2.$$

The base of the logarithm does not matter, as long as it is the same in the computation of m_{ℓ} and s_{ℓ} .

The test is based on the idea that, for an untruncated power law distribution, the logarithmic coefficient of variation of a sample is close to 1 (it is exactly equal to 1 in theory). The critical values of the test can be obtained simulating a power law distribution (the exponent does not matter) and calculating the distribution of cv_{ℓ} . In practice, this is equivalent to calculating the usual coefficient of variation (standard deviation divided by mean, without logarithms) of an exponential distribution with unit scale parameter, which is obtained from $-\ln(1-u)$, with u a uniform random number in $[0, 1)$. If the empirical value of the logarithmic coefficient of variation is between the percentiles 5th and 95th of the simulated values, the power law null hypothesis cannot be rejected, with a 90% confidence. If the logarithmic coefficient of variation is too small (below percentile 5), the power law must be rejected in favor of the lognormal, and if it is too high (above percentile 95) the power law is rejected, but the alternative is not the lognormal (this latter option does not happen in any of the cases analyzed here).

This simple test is the uniformly most powerful unbiased test for comparing the two alternatives and is rooted on the facts that the power law distribution is nested into the truncated lognormal and that their likelihood-ratio is a decreasing function of the logarithmic coefficient of variation (del Castillo & Puig, 1999). The former fact means that the power law can be understood as a special case of a truncated lognormal (with its parameters μ and σ fulfilling $\mu - \ln a \rightarrow -\infty$, $\sigma^2 \rightarrow \infty$, and $\beta = 1 + |\mu - \ln a|/\sigma^2$, taking into account that $\ln(x/a)$ is a truncated normal), and one evaluates whether the parameters of the lognormal are significantly different from the power law limit of the lognormal. So strictly speaking, one never rejects a lognormal but rejects a lognormal different than its power law limit. When performing the test for different values of k in order to find a transition from lognormal to power law (when increasing the cutting index k or the opposite transition when decreasing k), the test becomes somehow “subjective” as sometimes the crossing of the critical region is erratic. In any case, this will provide us with a value of the cutoff a , called now a_{cv} in order to distinguish it from the one coming from the fit, signaling the value above which a lognormal fit does not bring any improvement with respect an untruncated power law. In consequence, the range of variation of a in the previous section will be $a > a_{cv}$ (for the untruncated power law only). In some cases, although a power law tail cannot be rejected in front of the lognormal for some range, the lognormal will provide a much larger fitting range (beyond the tail) and will be therefore preferred.

Note that, in general, a likelihood-ratio test does not tell us if any of the two fits is good or bad; rather, it yields which one of the two options has higher likelihood and if the difference is significant or not. So, even if the power law is rejected in front of the lognormal, the latter can be a bad fit, or on the contrary, the power

Table 1
Results of the Untruncated Power Law Fit

Data set	N	Units	$x_{(N)}$	a_{fit}	r	n	β	p	a_{cv}
EQ CMT global	48,636	dyn cm	$5.3 \cdot 10^{29}$	$4.0 \cdot 10^{27}$	2.12	97	2.087	0.33	$*2 \cdot 10^{27}$
EQ California	179,255	dyn cm	$1.1 \cdot 10^{27}$	$1.5 \cdot 10^{21}$	5.89	2,883	1.655	0.30	$3 \cdot 10^{20}$
TD Florida	163,019	km ²	45.7	1.0	1.66	476	2.472	0.39	0.8
SH Kentucky	101,095	km ²	31.3	0.2	2.16	511	2.485	0.77	0.2
SH Dead Sea	1,033	km ²	0.0041	0.00044	0.98	48	2.804	0.59	0.0002
Fires Angola	17,643	ha	271,000	63	3.63	1,294	1.818	0.22	30
Fires Canada	408	ha	67,600	12,600	0.73	13	2.277	0.25	$*10,000$
TC Natl	771	$10^{10} \text{ m}^3/\text{s}^2$	25	12.6	0.31	16	5.145	0.22	$*10$
TC EPac	594	$10^{10} \text{ m}^3/\text{s}^2$	31	5.0	0.79	76	3.275	0.35	5
TC Natl+EPac	1,065	$10^{10} \text{ m}^3/\text{s}^2$	31	7.9	0.59	56	3.578	0.55	$*8$
Rain CA	5,037,333	km ²	238,000	100,000	0.38	165	6.479	0.50	100,000
TP land	6,385,195	km ³	177	33	0.73	286	4.109	0.38	30
TP ocean	10,372,063	km ³	2,080	200	1.02	555	3.250	0.47	$*200$
TP land+ocean	16,757,258	km ³	2,080	200	1.02	555	3.250	0.47	$*200$
Fireballs	748	kt	440	0.3	3.14	278	2.022	0.21	0.2

Note. The data sets contain N events, the maximum value of the variable is $x_{(N)}$, the number of data in the power law range is n , the lower cutoff of the fit is a_{fit} , the exponent is β , and the p value is p . The logarithmic range of the fit or number of orders of magnitude is $r = \log_{10}(x_{(N)}/a_{\text{fit}})$. The number of simulations is 1,000, and 50 values of a_{fit} , equispaced in logarithmic scale, are swept for each order of magnitude. The approximated value of the transition from lognormal to power law tail is also included and denoted a_{cv} . When this value is marked by an asterisk (in the rightmost column), it means that in principle (when no restriction was applied on a_{fit}) we found $a_{\text{cv}} > a_{\text{fit}}$ then we enforced $a_{\text{fit}} > a_{\text{cv}}$. In the rest of cases this was not required. EQ, TD, SH, TC, CA, and TP denote earthquakes, topographic depressions, sinkholes, tropical cyclones, rain cluster areas, and rain total precipitation, respectively. CMT = centroid moment tensor.

law can be a good fit and the lognormal an even better one. The likelihood-ratio test presented here, based on the logarithmic coefficient of variation of the tail, has the peculiarity that it does not need the calculation of the fitting parameters; this is an advantage from the computational point of view, as its implementation is very simple, but if one is interested in the parameters, these have to be obtained separately. Then, in order to obtain the truncated lognormal fits, we proceed in a way totally analogous as for the truncated power law (sweeping different values of a , applying Kolmogorov-Smirnov goodness of fit test, etc.).

4. Data and Results

The phenomena analyzed in this paper and their corresponding data sets are described below. Complete information about the outcome of our statistical analysis is provided in Tables 1-6. Table 1 shows the results of the fitting of an untruncated power law distribution. Table 2 complements these results with the uncertainty of the parameters obtained from bootstrap. Table 3 shows the results for a truncated lognormal, only for the data sets for which this distribution yields a better fit than the untruncated power law. Table 4 corresponds to the fitting of a truncated power law, only when this distribution leads to a different fit than the untruncated case. Table 5 gives the uncertainty obtained by bootstrap of the resulting parameters. Table 6 summarizes the results with the preferred distribution for each data set.

Figures 1 and 2 display the empirical distributions together with the preferred fits in each case. These figures play no role in the fitting procedure and are shown only for the sake of illustration, to have a visual and intuitive perspective. The empirical distributions are properly normalized; the fits, as defined in general over a smaller range, are not normalized but adapted to the normalization of the empirical distributions (see the captions for detailed information).

4.1. Earthquakes

As mentioned in section 1, earthquake size distributions have been related to power laws since the 1930s (Utsu, 1999). In 1944 Gutenberg and Richter published their celebrated relation for the number of earthquakes in terms of their magnitude (Gutenberg & Richter, 1944), which turns out to be an exponential

Table 2
Application of the Bootstrap Procedure to the Untruncated Power Law Fit

Data set	a_{fit}	$\bar{\beta} \pm \sigma_b$	\bar{p}		
EQ CMT global	$2.6 \cdot 10^{27}$	$4.4 \cdot 10^{27}$	$7.4 \cdot 10^{27}$	2.05 ± 0.16	0.35
EQ California	$2.1 \cdot 10^{21}$	$7.2 \cdot 10^{21}$	$2.6 \cdot 10^{22}$	1.65 ± 0.04	0.29
TD Florida	0.52	1.0	1.9	2.50 ± 0.16	0.33
SH Kentucky	0.07	0.2	0.5	2.47 ± 0.24	0.33
SH Dead Sea	$2.4 \cdot 10^{-4}$	$4.5 \cdot 10^{-4}$	$8 \cdot 10^{-4}$	2.89 ± 0.66	0.32
Fires Angola	40	120	370	1.79 ± 0.07	0.29
Fires Canada	12,000	15,300	19,500	2.85 ± 0.65	0.30
TC NAtl	11.1	12.6	14.4	5.88 ± 1.62	0.39
TC EPac	4.7	6.5	8.9	3.89 ± 1.14	0.38
TC NAtl+EPac	8.0	10.8	14.7	4.54 ± 1.61	0.41
TP land	27	34	44	4.29 ± 0.57	0.38
TP ocean	190	270	380	3.47 ± 0.31	0.40
TP land+ocean	190	270	380	3.47 ± 0.31	0.40
Fireballs	0.4	0.6	1.0	1.95 ± 0.35	0.37

Note. The exponent β is represented by the mean of all bootstrap results, $\bar{\beta}$, and variability in β by 1 standard deviation σ_b . The p value is also given in terms of the mean value \bar{p} . The variability of lower cutoff a is calculated by taking its logarithm, calculating the mean and the standard deviation, and transforming back taking the exponential of the results. The three values reported are associated to the mean of the logarithm and to this ± 1 standard deviation. The number of bootstrap samples is 100.

relation (some literature shows a certain confusion when mentioning “power law earthquake magnitudes”). The reason for the exponential relation is that magnitude is a logarithmic measure of size, for example, magnitude is proportional to the logarithm of energy (Kanamori & Brodsky, 2004) and when the Gutenberg-Richter relation is represented in terms of a more physical size (energy, seismic moment, rupture area, etc.) a power law should be recovered (Burrige & Knopoff, 1967). The Gutenberg-Richter relation, or law, has revealed as a very robust pattern of earthquake occurrence, and it has been claimed that their power law exponent turns out to be nearly universal, in the sense that for many regions of the world and for different ranges of sizes, it takes values close to $5/3 \approx 1.67$ (Godano & Pingue, 2000; Kagan, 1999; 2002; 2010). However, other authors have claimed systematic variation of the power law exponent (Schorlemmer & Wiemer, 2005), which may be related to different tectonic stress regimes (Schorlemmer et al., 2005).

Some authors have argued that an untruncated power law distribution is problematic, as extrapolation of this relation to the largest earthquakes would lead to an infinite release of energy in the long term, due to the divergence of the mean value of power law distributions when $\beta \leq 2$ (Knopoff & Kagan, 1977; Serra & Corral, 2017). So deviations from the Gutenberg-Richter power law behavior should be expected for the largest earthquakes; nevertheless, we will show that the untruncated power law is not such a bad model for earthquake sizes.

Table 3
Results of the Lognormal Fit for the Data Sets for Which This Leads to Better Results than the Untruncated Power Law, in the Sense that the Fitting Range is Remarkably Larger

Data set	N	a_{fit}	b_{fit}	r	n	μ	σ	p
TD Florida	163,019	0.018	∞	3.40	35,167	-9.85	2.84	0.59
SH Kentucky	101,095	0.0095	∞	3.51	17,624	-9.70	2.54	0.22
SH Dead Sea	1,033	$1.3 \cdot 10^{-6}$	0.005	3.60	964	-10.4	1.64	0.23
Fires Angola	17,643	8.7	∞	4.49	5,349	-13.2	4.96	0.32
Fires Canada	408	3.3	∞	4.3	314	3.36	3.29	0.45

Note. The μ and σ are the lognormal parameters; note that other researchers prefer to report e^μ and e^σ instead (Limpert et al., 2001). The upper cutoff is fixed to $b^{-1} = 0$, except for the Dead-Sea sinkholes. The number of simulations is 1,000, and 50 values of a_{fit} , equispaced in logarithmic scale, are swept for each order of magnitude.

Table 4

Results of the Truncated Power Law Fit, Only for the Data Sets Which Lead to Power Law Ranges Clearly Different Than the Untruncated Case

Data set	N	a_{fit}	b_{fit}	r	n	β	p
EQ CMT global	48,636	$1.3 \cdot 10^{24}$	$2 \cdot 10^{27}$	3.20	22,061	1.655	0.46
SH Dead Sea	1,033	$2.5 \cdot 10^{-7}$	$1.3 \cdot 10^{-5}$	1.7	323	0.391	0.24
Fires Canada	408	1.0	12,600	4.1	395	1.153	0.23
TC NAtl	771	0.16	10	1.8	534	1.224	0.27
TC EPac	594	0.08	10	2.1	511	1.085	0.37
TC NAtl+EPac	1,065	0.16	10	1.8	777	1.156	0.26
Rain CA	5,037,333	6,310	50,100	0.9	15,817	1.711	0.32
TP ocean	10,372,063	0.126	12.6	2.0	1,273,883	1.721	0.66

Note. The number of data in the truncated power law range is n , the lower cutoff of the fit is a_{fit} , the upper cutoff is b_{fit} , the exponent is β , and the p value is p . The number of orders of magnitude covered by the fit is $r = \log_{10}(b_{\text{fit}}/a_{\text{fit}})$. The number of simulations is 1,000 (except for the case of total precipitation of ocean rain clusters, which is 100), and 10 values of a_{fit} are swept equispaced in logarithmic scale for each order of magnitude.

We analyze the centroid moment tensor catalog (Ekström et al., 2012), which records (among other variables) the seismic moment of earthquakes across the globe (so x is the seismic moment, measured in dyn cm, noting that $1 \text{ dyn cm} = 10^{-7} \text{ N m}$). The temporal period of our study goes from 1 January 1977 to 21 August 2017. A refined analysis would have separated shallow, intermediate, and deep events or, even better, different tectonic zones (Kagan et al., 2010); however, we have considered the overall catalog. In addition, we also analyze seismicity from Southern California (USA), using the catalog of Yang et al. (2012), which covers the 30-year period 1981–2010, contains focal mechanisms, and includes the moment magnitude m , which can be directly converted to seismic moment x (in dyn cm) by means of the formula (Hanks & Kanamori, 1979):

$$x = 10^{1.5m+16.1}.$$

The logarithmic coefficient of variation test applied to the centroid moment tensor catalog indicates that an untruncated power law distribution is not preferred in front of a lognormal for a cutoff a smaller than $2 \cdot 10^{27}$ dyn cm (corresponding to 7.5 in moment magnitude). So the power law fitting procedure with a restricted to be above this value leads to $\beta \simeq 2.1$, for 2 orders of magnitude (this is significantly different than the usual value $\beta \simeq 5/3$). Nevertheless, this does not preclude that other distributions can fit the data even better (Serra & Corral, 2017). In any case, the lognormal is not one of this, and no lognormal fit is found. The fit of a truncated power law restricted to upper cutoffs b below the crossover value $2 \cdot 10^{27}$ dyn cm leads this time to the usual value, namely, $\beta = 1.655$, for 3 orders of magnitude (with a lower cutoff corresponding to 5.3 in moment magnitude). As the fitting ranges of both power laws (untruncated and truncated) almost overlap, we can conclude that a double power law distribution with a crossover at 7.6 in magnitude is a satisfactory result; this is in agreement with previous literature (Pacheco et al., 1992; Yoder et al., 2012). This

Table 5

Application of the Bootstrap Procedure to the Truncated Power Law Fit

Data set	a_{fit}			b_{fit}			$\bar{\beta} \pm \sigma_b$	\bar{p}
EQ CMT global	$1.2 \cdot 10^{24}$	$3.2 \cdot 10^{24}$	$8.9 \cdot 10^{24}$	$1.0 \cdot 10^{27}$	$1.6 \cdot 10^{27}$	$2.6 \cdot 10^{27}$	1.66 ± 0.02	0.34
Fires Canada	1.5	7.1	33	9,400	27,000	78,000	1.21 ± 0.08	0.29
TC NAtl	0.06	0.14	0.35	2.1	6.1	17	1.16 ± 0.25	0.31
TC EPac	0.06	0.10	0.17	3.8	7.9	17	1.08 ± 0.12	0.30
TC NAtl+EPac	0.06	0.14	0.30	2.0	6.4	20	1.08 ± 0.26	0.32
TP ocean	0.08	0.27	0.91	2.5	6.3	16	1.73 ± 0.03	0.35

Note. Only cases which lead to meaningful power laws are included. The exponent β is represented by the mean of all bootstrap results, $\bar{\beta}$, and variability in β by 1 standard deviation σ_b . The p value is also given in terms of the mean value \bar{p} . The variability of both cutoffs a and b is calculated as in the untruncated case by the mean ± 1 standard deviation of their logarithms. The number of bootstrap samples used is 100, except for the total precipitation over the ocean, which is 30.

Table 6
Summary of Results Showing the Preferred Distribution for Each Data Set

Data set	Preferred distribution
EQ CMT global	Double power law
EQ California	Untruncated power law
TD Florida	Truncated lognormal
SH Kentucky	Truncated lognormal
SH Dead Sea	Truncated lognormal (with $b^{-1} \neq 0$)
Fires Angola	Truncated lognormal
Fires Canada	Truncated power law + truncated lognormal
TC NATl	Truncated power law
TC EPac	Truncated power law
TC NATl+EPac	Truncated power law
Rain CA	None
TP land	None
TP ocean	Truncated power law
TP land+ocean	None
Fireballs	Untruncated power law

Note. For the Canadian wildfires, there is a truncated power law regime starting at the minimum x followed by a truncated lognormal covering up to the largest x , without a clear transition between both distributions.

double power law, in addition, avoids the problem of the divergence of the mean energy, as the exponent of the power law tail is $\beta_2 > 2$. On the other hand, the fitting of an untruncated power law to the whole range of the data would have not lead to the rejection of it ($\beta \approx 1.67$), due to the small weight of the deviations at the tail in front of the rest of the distribution. This case illustrates the convenience of using the test on the logarithmic coefficient of variation in order to guide the fitting procedure based on maximum likelihood and goodness of fit. For California we find an untruncated power law with $\beta = 1.655$ for almost 6 orders of magnitude, starting at $a = 1.5 \cdot 10^{21}$ dyn cm (3.4 moment magnitude). This constitutes the largest fitting range found in this article. The truncated power law leads to very similar results. Moreover, the lognormal fit is not preferred in this range, as indicated by the computation of cv_r and the corresponding test.

4.2. Karst Sinkholes and Closed Topographic Depressions

Sinkholes are ground depressions produced by subsidence due in most cases to karst, that is, by dissolution of soluble rocks by groundwater. Sinkholes pose a hazard since they may form under buildings and infrastructure (such as roads, railways, and pipelines) and are particularly dangerous if they collapse suddenly, causing even human casualties (Brinkmann, 2013; Galve et al., 2011).

Power law frequency-size relations have recently been proposed for sinkholes, considering either their diameter or their area as a measure of size (Galve et al., 2011; Wall & Bohnenstiehl, 2014; Yizhaq et al., 2017), and their exponents have been proposed to vary as new sinkholes develop, grow, and coalesce (Yizhaq et al., 2017). The frequency-size relation of topographic depressions in Florida shows a similar behavior (Wall & Bohnenstiehl, 2014). These depressions are used as proxies to karst features, albeit not all of them are sinkholes (Arthur et al., 2007). Notice that a logarithmic function between cumulative frequency and sinkhole diameter proposed for other sinkhole data sets (Gutiérrez et al., 2016; Taheri et al., 2015) is equivalent to a power law with unit exponent.

Sinkhole maps can be either delineated manually or by automatically identifying topographic depressions in digital elevation models, which may lead to differences in the resulting inventories (Wall et al., 2017). Here we use the Kentucky (USA) sinkhole database, mapped manually and probably the largest sinkhole data set available, with over 100,000 sinkholes (Paylor et al., 2003); the database of Florida (USA) closed topographic depressions, based on automatic mapping, comprising more than 160,000 depressions (Florida Department of Environmental Protection, 2004); and a compound data set of more than 1000 sinkholes

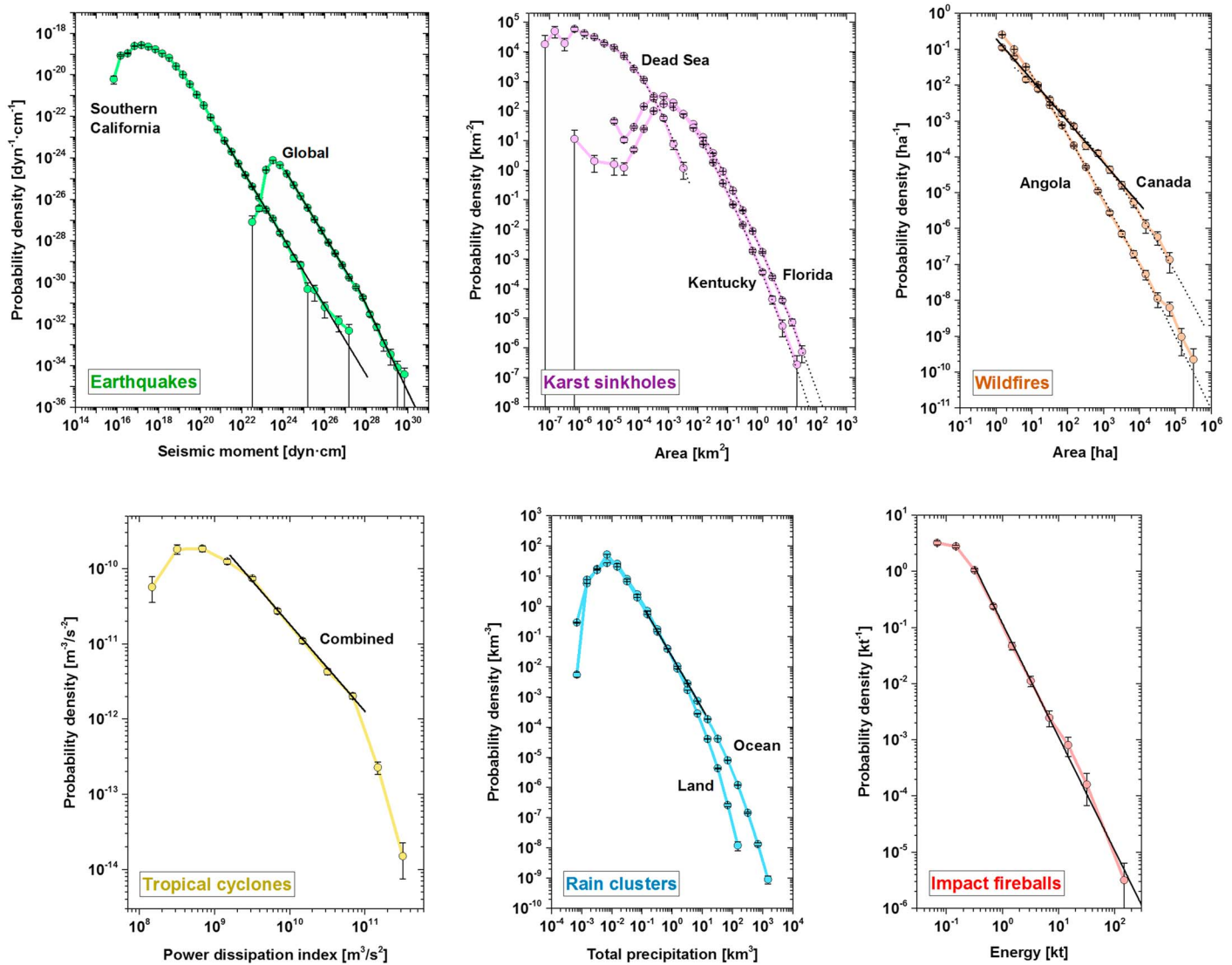


Figure 1. Estimation of empirical probability densities of size together with the preferred fits for some of the data sets analyzed in this study. Solid lines indicate power law fits and dashed lines lognormal fits. The theoretical distributions are rescaled as $n f(x)/N$ in order to properly fit the representation of the empirical distributions, which are normalized over a different range. The uncertainty of the empirical density represents one standard deviation (Deluca & Corral, 2013).

next to the Dead Sea (Yizhaq et al., 2017). The size is measured in terms of the area ($x = A$), in square kilometers. Sinkholes may have a minimum area on the order of 0.1–1 m^2 , which is observed in the Dead Sea database and in other detailed studies (Galve et al., 2009). In contrast, for the Kentucky and Florida databases, the smallest reported areas are expected to be limited by the resolution of the maps used for their compilation. Meanwhile, the largest sinkhole size mapped may be affected by border effects, especially in small geographic areas.

Our results show that the two largest data sets (Florida and Kentucky), although not corresponding exactly to the same geological phenomenon, lead to similar results. An untruncated power law distribution can be fit for 1.5 and 2 orders of magnitude, respectively, with exponent β very close to 2.5. The cv_r test confirms these results, in the sense that in the resulting range the power law fit is preferred in front of the lognormal. However, as the lognormal holds for a much larger range, this distribution is, overall, preferred, with $\mu \simeq -10$ and $\sigma \simeq 2.5$ –2.8. Results for the truncated power law distribution are similar to the ones of the untruncated case, with a somewhat smaller exponent ($\beta \simeq 2.3$) for Kentucky. A spurious power law that appeared for the Florida data in the range of very small areas has been disregarded.

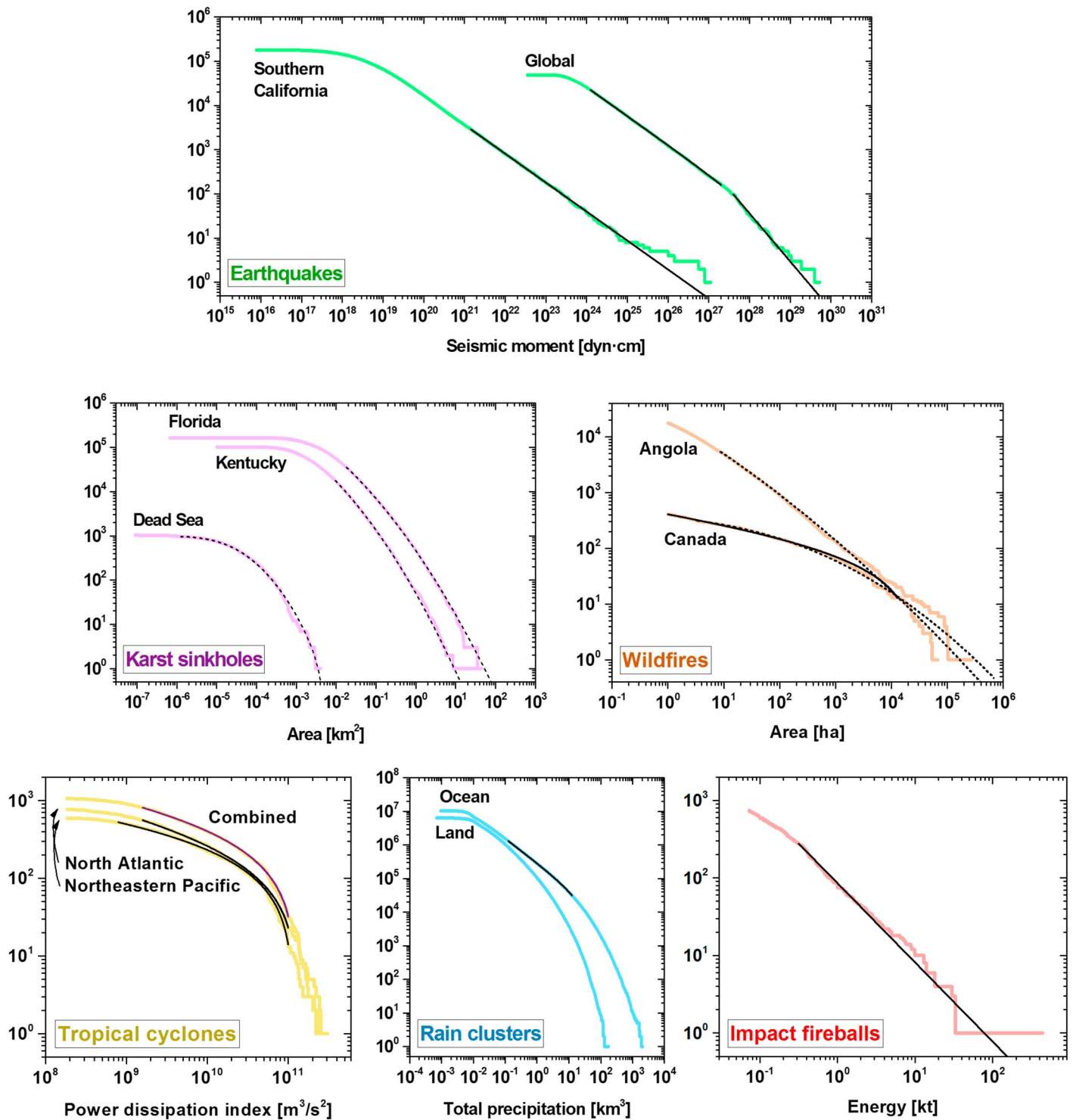


Figure 2. Number of structures or events with “size” larger or equal than the value of x pointed in the axis, together with the preferred fits for all data sets analyzed in this study (except for the area of rain clusters and the total precipitation by clusters over land+ocean, which lead to no fit; the total precipitation over land is included for visual comparison with the ocean case). Solid lines indicate power law fits and dashed lines lognormal fits. Note that truncated power laws can be far from linear in the log-log plots, especially for tropical cyclones. In order to properly fit the empirical results, the fits need to be rescaled and shifted as $nS(x) + NS_{\text{emp}}(b)$, with $NS_{\text{emp}}(b)$ the number of data with size at b or larger.

The description of the Dead Sea data set in terms of the power law is poorer. An untruncated power law distribution is not rejected for the last order of magnitude (being generous) but with less than 50 data points and with a larger exponent ($\beta \simeq 2.8$). The logarithmic coefficient of variation confirms this range for which the lognormal tail is not preferred; nevertheless, as the lognormal leads to a much larger fitting range, the latter is preferred to describe the distribution globally. In this case, though, the lognormal needs an upper cutoff, $b \simeq x_{(N)}$ (otherwise, for $b \rightarrow \infty$, the lognormal is rejected).

On the other hand, note that if the areas A are transformed into linear dimensions L by means of the relation $L \propto A^{1/2}$, equation (6) with $z = 2$ indicates that a range of β from 2.5 to 2.8 transforms to the range 4–4.6 for β_L .

4.3. Wildfires

Forest-fire models were one of the most popular topics in the field of self-organized criticality; however, as far as we know, simulation results from these toy models were not contrasted with observational data until the work of Malamud et al. (1998). Before the self-organized criticality epoch, fire size distributions had been plotted by Minnich (1983). Malamud et al. (1998) found that areas burned by wildland fires in different places of the United States and Australia (including paleofire records) follow (untruncated) power law distributions with exponent β ranging from 1.3 to 1.5. Later, Malamud et al. (2005) studied 18 different ecoregions of the United States, finding power law distributions with exponents from 1.3 to 1.75. Many other statistical studies have been performed; see, for instance, the citations of Malamud et al. (2005). Interestingly, some authors have claimed that burned areas in other regions are better described by the lognormal distribution (Corral et al., 2008; Hantson et al., 2016).

Hantson et al. (2016) generated burned-area maps of high resolution (30 m) from satellite (Landsat) imagery, for some of the most important fire occurrence regions in the world. The resulting database comprised eight regions from different ecosystems and climates, in all continents (except Antarctica). The burned area A , in ha (1 ha = 0.01 km²), was used as a measure of fire size ($x = A$). After their careful statistical analysis, the authors found that only two regions were compatible with the truncated power law hypothesis (in Canada and Kazakhstan), with exponents β equal to 1.0 and 1.3, respectively. Four other sites showed a lognormal behavior, whereas the remaining two (in Angola and Australia), were not compatible with any of the two statistical models. Here we select as representative sites those at Angola and Canada, and we reanalyze their wildfire records. The former site is associated to open woodland, with data gathered along 4 (nonconsecutive) years, whereas the Canada data correspond to boreal forest monitored for 14 years.

In contrast to the original results, our analysis shows that the wildfire data from Angola can be well represented both by an untruncated power law and by a lognormal distribution. The untruncated power law holds for burned areas greater than about 60 ha (corresponding to more than 3.5 orders of magnitude), with an exponent $\beta \simeq 1.8$. In the comparison with the lognormal fit, the power law is not rejected in this range. However, the lognormal is valid for a larger range, starting at about 10 ha, covering 4.5 orders of magnitude and comprising more than 4 times the number of points comprised by the power law. The fit of the truncated power law distribution does not lead to remarkable differences with respect to the untruncated power law. Therefore, the lognormal is the preferred distribution.

In contrast, the Canada data yield a very short power law tail, with a larger exponent and for a more limited range, starting at about 12,000 ha and containing very few data points. We can disregard this power law as spurious and embrace the lognormal fit which is valid for $x \geq 3.3$ ha up to the largest value (67,000 ha) and covers a significant part of the data (77% of all data points). In addition, and in agreement with the original work, a truncated power law with $\beta \simeq 1.15$ gives a good fit between 1 and 12,000 ha, covering 97% of all data points. As the truncated power law and the lognormal are defined over different ranges we have no way to decide between them, and we consider the two fits as valid. That is, we can say that the truncated power law holds for small x and the lognormal for large x but without a clear transition between them.

These results, together with those of many other previous researchers, make it clear that, in contrast to earthquakes, wildfires cannot be characterized by nearly universal power law exponents, as originally noticed in a qualitative way by Minnich (1983).

4.4. Tropical Cyclones

The term tropical cyclone applies to hurricanes and typhoons, which are the same phenomenon, with the only difference that the former happens in the North Atlantic and the Northeast Pacific and the latter in the

Northwest Pacific. But the term also comprises weaker systems, as tropical storms and tropical depressions. The categorization is established by the maximum sustained wind speed, which in tropical depressions is less than 34 knots and in tropical storms is between 34 and 64 knots (1 knot = 0.5144 m/s); otherwise, the tropical cyclone is considered a hurricane or a typhoon (or a severe tropical cyclone or a severe cyclonic storm, in other ocean basins) (Emanuel, 2005a).

Emanuel (2005b) introduced the so-called power dissipation index (PDI) as a rough estimation of the energy released by tropical cyclones in some ocean basin during a whole tropical cyclone season. Later, the PDI was applied to estimate the energy of individual tropical cyclones (Corral et al., 2010). It is defined as

$$PDI = \sum_{j=1}^K v_j^3 \Delta t,$$

where the index j denotes the K different records of a tropical cyclone, at different times, separated by intervals of $\Delta t = 6$ hr and v_j is the maximum sustained wind speed of record j . We will use then the PDI as a measure of tropical cyclone size (that is, $x = PDI$) and will convert the PDI units to cubic meter per square second, although a rough conversion factor to Joules has been proposed (PDI multiplied by $5 \cdot 10^6$ should yield energy in Joules) (Corral & Turiel, 2012; Emanuel, 1998). A truncated power law distribution of PDI was previously proposed (Corral et al., 2010).

Tropical cyclone records analyzed here correspond to the North Atlantic (NAtl) and the Northeastern Pacific (EPac) basins, for the periods 1966–2016 and 1986–2016, respectively, and are obtained from the NOAA (USA) HURDAT2 data set (Atlantic Oceanographic and Meteorological Laboratory, 2018). We also consider an aggregated data set joining the two basins (NAtl+EPac), for the period 1986–2016. A map view of the trajectories of the tropical cyclones in both basins indicates that it may make sense to consider the two basins together, as a single unified mega-basin, in some sense.

In all three cases we find that an untruncated power law may fit the tail of the distributions, with exponent β around 4 or larger, with great uncertainty (as shown by bootstrap). Nevertheless, this power law is rather marginal, as it extends for less than 1 order of magnitude; in addition, the increase of the apparent value of the exponent with a shows that we are not dealing with a genuine power law. Notice that the power law exponent of the joined data set does not fulfill the law of harmonic means reported previously (Navas-Portella et al., 2018), because the fitting ranges of each data set are somewhat different. Nevertheless, the lognormal fit is not preferred for the tail. Other works have fit a truncated gamma distribution (which contains an exponential tail) to this kind of data (Corral & Turiel, 2012; del Castillo et al., 2017). When fitting a truncated power law, the results are in agreement with the original reference (Corral et al., 2010), with an exponent β in the range 1.1–1.2, for about 2 orders of magnitude. On the other side, a truncated lognormal distribution with $b \rightarrow \infty$ does not fit the data. Finally, note that, from the figure and the conversion factor presented above, the most extreme tropical cyclones (in terms of energy) release an energy around $3 \times 10^{11} \text{ m}^3/\text{s}^2 \simeq 1.5 \times 10^{18} \text{ J}$.

4.5. Rain

Rainfall has been traditionally studied in terms of rain collected during a fixed time period (1 day or 1 month) at a single site (i.e., a point measure in space). Peters and coauthors (Peters et al., 2002; Peters & Christensen, 2002; 2006), and previously Andrade et al. (1998), challenged that approach, defining the rain event over some site as a continuum of rain occurrence in time. In the ideal case, one should be able to measure rain with high resolution in time, for instance, 1 min. In this way, for a single site in the Baltic Sea, Peters et al. (2002) obtained a power law exponent $\beta \simeq 1.35$ for the total rain collected during rain events. A subsequent analysis for different sites of the globe, where rain was recorded using different instruments, found a nearly universal exponent β in the range 1.0–1.2.

Later, Peters et al. (2012) took a different view, defining the rain event not along time but across space, that is, they considered the instantaneous area of precipitation clusters. This was obtained as in percolation theory, aggregating nearest-neighbor precipitating pixels corresponding to one time slice. The resulting areas A , in square kilometers were measured (i.e., $x = A$). The data used came from the precipitation radar of the Tropical Rainfall Measuring Mission satellite. Peters et al. (2012) noticed a power law-like regime for the areas, with exponent $\beta \simeq 2.05$. In fact, a similar result was claimed much earlier by Lovejoy (1981) for (radar) rain areas in the tropical Atlantic, stating power law behavior with $\beta \simeq 1.82$. Few years later Lovejoy and Mandelbrot (1985) reported $\beta \simeq 1.75$ in the same context.

Our reanalysis of Peters et al.'s (2012) data shows that the fit of an untruncated power law distribution leads to poor results. The power law can only be fit to the most extreme events, comprising less than 200 data points (out of more than 5 million) and covering less than half an order of magnitude. Moreover, the apparent exponent shows an increase with the cutoff value. The truncated power law fit does not lead either to very positive results, despite the fact that the graphical representation of the distribution shows a decreasing linear trend in a log-log plot. The reason of this failure may be due to the astronomically large number of clusters. This means that the uncertainty associated with the empirical distribution is very tiny, and the goodness of fit test can detect the smallest differences with respect a real (ideal) power law behavior. The best truncated power law obtained (the one having larger ratio b/a) holds for less than 1 order of magnitude and comprises less than 1% of the clusters, showing significant variation with the change of a and b ; thus, we disregard the obtained power law as not relevant.

More recently, Traxl et al. (2016) obtained the total volume of precipitated water in rain events defined over space and time. They employed the Tropical Rainfall Measuring Mission records, calculated in space time cells with a resolution of 3 hr in time and 0.25° in (two-dimensional) space, covering the globe from -50° to 50° in latitude, for the time period 1998–2014. Spatiotemporal rain clusters were defined via next-nearest neighboring “occupied” cells in space and nearest neighbors occupied cells in time (with a total of 26 neighbors per cell). Cell occupation was understood as occupation by extreme rain, that is, with high rain rates, above certain rain-rate thresholds. These thresholds were defined locally, using the per-cell 90th percentile of rain rate (restricted to values above 0.1 mm/hr). The resulting thresholds ranged from 2 to 10 mm/hr. The volume of rain for each cluster, measured in cubic kilometers, was calculated by integrating the rain rate over the spatiotemporal cluster. In a formula,

$$V = \int_{\text{cluster}} R dS dt$$

(so $x = V$), where the integral is understood as summation over the cells with the mentioned resolution and R is the rain rate defined over space (dS) and time (dt). We stress that V is not the spatial volume of the cluster but the volume of rain precipitated by the spatiotemporal cluster. Notice that one can convert precipitated volume into energy through the latent heat of condensation of water (approximately 2,500 J/g); thus, 1 km^3 of precipitation is roughly equivalent to 2.5×10^{18} J of latent heat release. Precipitation depth measured by Peters et al. (2002, 2010) can be transformed into energy per unit area by means of $1 \text{ mm} \approx 2.5 \times 10^6 \text{ J/m}^2$.

The resulting rain events were classified into two groups: land events (with 90% or more of their cells corresponding to land) and ocean events (defined in an analogous way); the rest of clusters (2.5% of the total) were disregarded. The authors obtained that a truncated gamma distribution (called truncated power law by them) is what better fitted the ocean data set, whereas the Weibull distribution (called there stretched exponential) fitted both the land data set and the aggregated land+ocean data set. The corresponding power law exponent given by the gamma distribution was $\beta \approx 1.71$ (the Weibull distribution does not have a clear power law regime when its shape parameter goes to zero, which is what the authors found).

We reanalyze the data of Traxl et al. (2016), kindly updated by the authors for the 20-year period 1998–2017. The land and ocean data sets were defined by 80% or more cells in there. Our results for the untruncated power law fit lead to very short power law tails (1 order of magnitude or less) with values of β rather large (again, the bootstrap method shows large variability in these values, and a dependence of β on a is also present). The tail of the combined data set land+ocean is constituted exclusively by ocean events and leads to the same results as the ocean data set. The logarithmic coefficient of variation test indicates that the lognormal fit is not preferred for those short tails.

On the other side, for the ocean clusters, a truncated power law distribution with exponent $\beta = 1.7$ holds for 2 orders of magnitude, comprising more than 1 million data points. As far as we are aware, this is one of the power law distributions with more data ever found (Clauzet et al., 2009) using rigorous statistical procedures. The other two files do not show any truncated power law behavior, due to the great amount of data (taking smaller random subsamples, one may find that truncated power laws are accepted, as well as lognormal tails, but that would mean disregarding the majority of data). Regarding the overall shape of the probability density, it is a remarkable fact that this displays a great similarity with the probability density of the PDI of tropical cyclones (Corral et al., 2010), both shown in Figure 1. Note from there that the energy released by the most extreme rainfall events is of the order of $2 \times 10^3 \text{ km} \approx 5 \times 10^{21} \text{ J}$. This large difference

with respect to tropical cyclones may be due to the fact that in that case the energy referred to kinetic energy (Emanuel, 1998), whereas for rainfall we consider total latent heat released.

The reason of the difference between our results and those of the original reference (Traxl et al., 2016) is that these authors were comparing different distributions by means of likelihood-ratio tests but without testing the goodness of fit of any of the distributions individually. So they determine a relative comparison about which distribution is preferred in comparison with the others, but they do not provide absolute judgements.

4.6. Impact Fireballs

Fireballs are exceptionally bright meteors produced by the impact of asteroids or comets on Earth's atmosphere and are usually called bolides if they explode midair. Large enough impact air bursts, even if the impactor does not reach the surface, can produce damage and casualties by a variety of mechanisms, especially by wind blast, thermal radiation, and atmospheric shock wave overpressure (Rumpf et al., 2017), being the latter recently illustrated by the damaging 2013 Chelyabinsk impact (Brown et al., 2013; Heimann et al., 2013; Popova & the Chelyabinsk Airburst Consortium, 2013).

The distribution of energy of asteroid and comet impacts with Earth is usually reported as a power law (Boslough et al., 2015; Brown et al., 2013) composed by different data sets which span different parts of the energy range (from small meteors to fireballs to calculated impact rates from known near-Earth objects).

Here we use the fireball and bolide data provided by Center for Near Earth Object Studies (2018), based on reports by U.S. Government sensors (Boslough et al., 2015; Brown et al., 2002, 2013). The total impact energy (x) for each event is reported in kt (kilotons of TNT), extrapolated from the measured total optical radiated energy using an empirical fit (Brown et al., 2002). The largest fireball included there is Chelyabinsk (with a reported total energy of 440 kt), which was also independently located and characterized, even at regional or global distances, using the records of ground shaking produced by the shock wave (Brown et al., 2013; Heimann et al., 2013) and atmospheric infrasound (Le Pichon et al., 2013).

The data set includes events since April 1988, albeit, as other authors (Boslough et al., 2015; Brown et al., 2002, 2013) we use only the data since 1994, as earlier years are substantially incomplete. Until July 2018, the database contains 748 events. The percent of the Earth's surface covered by the sensors has varied over that period (Brown et al., 2002) and on average may be on the order of 80% for events with total energy > 1 kt (Brown et al., 2013).

Our statistical analysis shows that fireballs are well described by an untruncated power law distribution for about 3 orders of magnitude, with exponent $\beta \simeq 2$ but with large uncertainty. The truncated power law leads to practically the same results as the untruncated case. The fit of the lognormal distribution is also not rejected over more or less the same range as the power law; however, the cv_ρ test confirms that the power law is preferred in front of the lognormal distribution over that range.

5. Conclusions and Discussion

We have revisited the important problem of power law distributions in the size of geological and geophysical structures and of catastrophic phenomena of geoscience. Due to the delicate issues involved with power law fitting and the variety of approaches in the literature, we have undertaken a revision of some relevant examples of previously proposed power laws, in order to treat all systems within a unified framework and to facilitate the comparison between the results of different systems.

For that purpose, we have extended an existing method for fitting and goodness of fit testing of power law-like distributions. The important issue regarding these distributions is that the range over which a power law distribution may fit the data is unknown. The method, previously proposed by Peters et al. (2010) and Deluca and Corral (2013), uses the same tools as the so-famous procedure of Clauset et al. (2009) (maximum likelihood estimation and the Kolmogorov-Smirnov test) but is different in spirit, allowing the fitting of both untruncated and truncated power laws (generalization to other distributions is straightforward).

Three important improvements related with the cutoffs are included. First, for untruncated power laws the fitting range is constrained by a complementary likelihood-ratio test (based on the residual coefficient of variation) that compares a general power law tail with a general lognormal tail (Malevergne et al., 2011). Only lower cutoffs for which the power law is preferred in front of the lognormal are contemplated. Second, the variation of the apparent power law exponent with the cutoffs is studied in order to rule out spurious

power laws that appear when the number of data is low. And third, the uncertainty in the lower and upper cutoffs of the power law distributions is evaluated by bootstrap.

The results show a large diversity of outcomes. The energy released by impact fireballs is well fitted by an untruncated power law; nevertheless, as the size of the database is low, this result could change if much larger databases become available. An important issue here is the completeness of the records for all impact energies or at least the proper evaluation of incompleteness for the different energy ranges.

For the seismic moment of global earthquakes, we find two power law regimes, the first ranging up to about 7.6 in moment magnitude, with the usual exponent $\beta = 1.655$, and the second power law defined above the previous value, with exponent $\beta \approx 2$. This was previously proposed by some authors, due to geometric constraints of earthquake ruptures above that threshold magnitude, such as Pacheco et al. (1992) and Yoder et al. (2012). In contrast, Southern California seismicity shows a unique untruncated power law range, starting at around 3.4 in moment magnitude. This value, which can be interpreted as a measure of the completeness threshold of the analyzed catalog, may seem to be somewhat large, but let us recall that our fitting procedure is rather demanding, rejecting any power law fit whose p value is below 0.20. Indeed, the value is coincident with the independent estimates of the detection threshold of the Southern California Seismic Network during the period considered (Schorlemmer & Woessner, 2008). Despite the relatively large completeness threshold, we find the resulting power law holds for almost 6 orders of magnitude (for seismic moment), which is a rather impressive result.

Energy of tropical cyclones in two different ocean basins (Corral et al., 2010) is found to display truncated power law behavior over the central part of their distributions. Here, problems at small energies are especially important due to incompleteness of the records for small storms, whereas the largest events (the most extreme hurricanes) are strongly influenced by the boundary conditions imposed by the finite size of the basins over which they develop. Note that the size measure used here is a proxy for the cyclone energy, while the cyclone radius (influenced by other factors, see Chavas et al., 2016), is not necessarily correlated with the energy. The small size of the tropical cyclone databases does not allow to guarantee that the power law behavior is maintained if much larger records become available in the far future.

Rainfall clusters (Peters et al., 2012; Traxl et al., 2016) are in the opposite side of the spectrum regarding the number of data, which is “astronomical.” Except in one case, we are unable to find meaningful power law or lognormal fits. The reason, naturally, is the millions of events comprising the databases, which make almost impossible for goodness of fit test to accept (i.e., not reject) any proposed distribution. The remarkable exception is that of the total precipitation released by spatiotemporal rainfall clusters over the oceans (Traxl et al., 2016), for which we find a truncated power law ranging only for two decades but comprising more than 1 million data points. We are not aware of a power law distribution established with rigorous statistical protocols containing more points.

On the other hand, sinkholes and topographic depressions (Florida Department of Environmental Protection, 2004; Paylor et al., 2003; Yizhaq et al., 2017) are better described by truncated lognormal distributions, down to minimum area thresholds probably controlled by the resolution of the databases used. Although power law tails may fit narrow ranges of the largest areas reported, the lognormal distributions are preferred, as their fits cover a much larger range (including therefore a larger fraction of the entries contained in the catalogs).

The two examples of wildfires analyzed here (Hantson et al., 2016) are also well fitted by truncated lognormals over large ranges, although for the Canada record this is not incompatible with a power law regime (due in part to the low number of wildfires recorded there, both fits overlap over a significant range).

As this paper was pretended as an essentially statistical one, an issue that we have not considered so far is the physical reason behind power law distributions. Now we pay some attention to that before ending. For earthquakes and wildfires it is recognized that one feasible mechanism can be self-organized criticality (SOC) (Bak, 1996; Bak et al., 1987), as both phenomena are characterized by an activity front that propagates (somewhat fast) through a substrate, in an avalanche-like manner. The activation can be modeled as a branching process, but these processes only yield power law distributions if they are precisely at their critical point (Corral & Font-Clos, 2013). So the self-organization mechanism ensures that criticality is achieved “spontaneously” in these systems, through a balance between driving and dissipation, and so the substrate has to be at the onset of instability (all the time). But although the SOC mechanism is a plausible one for

these systems (Bak & Tang, 1989; Ito & Matsuzaki, 1990; Sornette & Sornette, 1989), it is an extraordinarily difficult task to establish that SOC is the responsible of power law size distributions in earthquakes, as there is a big gap in the simplicity of SOC models (Olami et al., 1992) and the enormous complexity of the real phenomenon.

Regarding wildfires, we have already seen (as some previous authors) that these seem to be better described by lognormals, at least for some particular data sets. We are not aware of modifications of SOC models that yield lognormal distributions, although the non-applicability of the SOC mechanism for wildfires in some cases was discussed by Pueyo et al. (2010). Notice also that the sinkhole model proposed by Yizhaq et al. (2017) was claimed to lead to power law distributions, although no goodness-of-fit was performed there and the results could be compatible also with the lognormal (remember that our preferred model in that case was lognormal). It is noteworthy that the lognormal distribution arises naturally for simple multiplicative random growth process, where the rate of growth is proportional to size multiplied by a random factor, as reviewed by Mitzenmacher (2004). This can easily be seen just applying the classical central limit theorem to evolution of the logarithm of the size.

The fact that power law distributions, similar to the Gutenberg-Richter law for earthquakes, also seemed to characterize rainfall led some authors to speculate that precipitation could be a sort of earthquake (avalanche) process in the sky (Peters et al., 2002; Peters & Christensen, 2002; 2006). The metaphor is very appealing, but we are not aware of any physical model of rainfall production in terms of avalanches (for an alternative explanation; see Dickman, 2003). Nevertheless, indirect proof has been gathered by the identification of a critical point in the transition to strong convection, to which the atmosphere seems to be “attracted” (Peters & Neelin, 2006). Interestingly, tropical cyclones are related to rainfall (they are a particular instance of it, an extreme case); so one can expect a connection between a SOC description of rainfall and a SOC description of tropical cyclones, although there are different options about which are the variables that would support the SOC description (Corral, 2010; Peters et al., 2012). For rainfall, one may consider that the release of energy takes place in the clouds, whereas for tropical cyclones one could locate the interaction in the ocean-air interface. Moreover, an important difference between tropical cyclones and earthquakes is that the former are dynamical and thermodynamical organized structures (one may talk about dissipative structures), whereas earthquakes lack this sort of machinery.

Needless to say, nowadays, it is well known that criticality and SOC are not the only mechanisms able to generate power law distributions (Mitzenmacher, 2004; Newman, 2005; Simkin & Roychowdhury, 2011; Sornette, 2004). A particularly simple but interesting alternative was proposed by Reed and Hughes (2002). In the context of Zipf's law, different power law-like models were proposed much earlier than SOC (Miller, 1957; Simon, 1955), like preferential growth or cumulative advantage (rich-get-richer) (Cattuto et al., 2007; Simon, 1955; Zanette, 2014; Zanette & Montemurro, 2005), which could make sense as well applied to growth processes in geophysics. Another interesting option, if the power law exponent is larger than 2, is stochastic differential equations with additive and multiplicative noises (Penland & Sardeshmukh, 2012; Sardeshmukh et al., 2015). However, other Zipf-like models are more difficult if not impossible to translate into geophysics (Corominas-Murtra et al., 2015; Ferrer-i-Cancho, 2016; Miller, 1957; Tria et al., 2014).

Finally, several authors have used some limit theorems in probability theory to justify the origin of power law distributions. For instance, the generalized central limit theorem ensures that when a fixed number of (independent and identically distributed) random variables are added, the result converges to a Lévy distribution if some conditions (that invalidate the application of the classical central-limit theorem) are fulfilled (Bouchaud & Georges, 1990). An analogous (but different) limit exists when the number of added random variables is not fixed but random, according to some prescribed distribution; the limit distributions for a geometric-distributed number of terms (geometric stable distributions) turn out to be the Mittag-Leffler distributions (Corral, 2009; 2015; Gnedenko & Korolev, 1996). In the same way, if instead of summing, one considers maximization, then the extremal types theorem applies, leading to the generalized extreme value distribution; and if one considers threshold exceedances and shifting, then the Pickands-Balkema-de Haan theorem leads to the generalized Pareto distribution (Coles, 2001). All these limit distributions contemplate power law-like tails; however, these tails are only obtained when the tails of the individual distributions (those that are added, maximized, etc.) are of the same kind. This fact excludes limit theorems as a genuine mechanism to generate power laws, as they ultimately deal with the trivial case of “power law-in, power

law-out,” in which a power law-like distribution is obtained from the input of another, unexplained, power law-like distribution.

Acknowledgments

We are very grateful to all researchers who have shared data with us: Alfredo Hernández, Abigail Jiménez, Víctor Navas-Portella, Patricia Paredes, Ole Peters, Salvador Pueyo, Dominik Traxl, and Hezi Yizhaq. John Wall provided valuable comments on sinkhole databases, and Pedro Puig and Isabel Serra provided statistical wisdom. Insight provided by the Editor (Cécile Penland) and the anonymous reviewers is also appreciated. We acknowledge support from the Spanish Ministry of Science, Innovation and Universities (projects FIS2015-71851-P, MAT2015-69777-REDT, Maria de Maeztu Program for Units of Excellence in R&DMDM-2014-0445, and Juan de la Cierva research contract FJCI-2016-29307 hold by A. G.). The data used in this paper are not original and have been provided by the authors quoted in the references and these acknowledgments.

References

Aban, I. B., Meerschaert, M. M., & Panorska, A. K. (2006). Parameter estimation for the truncated Pareto distribution. *Journal of the American Statistical Association*, *101*, 270–277.

Abramowitz, M., & Stegun, I. A. (Eds.) (1965). *Handbook of mathematical functions*. New York: Dover.

Adamic, L. A., & Huberman, B. A. (2002). Zipf's law and the Internet. *Gloittometrics*, *3*, 143–150.

Andrade, R. F. S., Schellnhuber, H. J., & Claussen, M. (1998). Analysis of rainfall records: Possible relation to self-organized criticality. *Physica A*, *254*, 557–568.

Arthur, J. D., Wood, H. A. R., Baker, A. E., Cichon, J. R., & Raines, G. L. (2007). Development and implementation of a Bayesian-based aquifer vulnerability assessment in Florida. *Natural Resources Research*, *16*(2), 93–107.

Aschwanden, M. (2013). SOC systems in astrophysics. In M. Aschwanden (Ed.), *Self-organized critical phenomena*. Berlin: Open Academic Press.

Atlantic Oceanographic and Meteorological Laboratory (2018). HURDAT2 Hurricane Database. Retrieved from <http://www.aoml.noaa.gov/hrd/hurdat/hurdat2-1851-2016-apr2017.txt>, <http://www.aoml.noaa.gov/hrd/hurdat/hurdat2-nepac-1949-2016-apr2017.txt>

Axtell, R. L. (2001). Zipf distribution of U.S. firm sizes. *Science*, *293*, 1818–1820.

Baddeley, A., & Vedel Jensen, E. B. (2005). *Stereology for statisticians*. Boca Raton: Chapman & Hall / CRC.

Baiesi, M., Paczuski, M., & Stella, A. L. (2006). Intensity thresholds and the statistics of the temporal occurrence of solar flares. *Physical Review Letters*, *96*, 51103.

Bak, P. (1996). *How nature works: The science of self-organized criticality*. New York: Copernicus.

Bak, P., Christensen, K., Danon, L., & Scanlon, T. (2002). Unified scaling law for earthquakes. *Physical Review Letters*, *88*, 178501.

Bak, P., & Tang, C. (1989). Earthquakes as a self-organized critical phenomenon. *Journal of Geophysical Research*, *94*, 15,635–15,637.

Bak, P., Tang, C., & Wiesenfeld, K. (1987). Self-organized criticality: An explanation of $1/f$ noise. *Physical Review Letters*, *59*, 381–384.

Barabási, A.-L. (2018). Love is all you need. Clauset's fruitless search for scale-free networks. unpublished. Retrieved from <https://www.barabasilab.com/post/love-is-all-you-need>

Baró, J., & Vives, E. (2012). Analysis of power law exponents by maximum-likelihood maps. *Physical Review E*, *85*, 66121.

Bauke, H. (2007). Parameter estimation for power law distributions by maximum likelihood methods. *European Physical Journal B*, *58*, 167–173.

Boffetta, G., Carbone, V., Giuliani, P., Veltri, P., & Vulpiani, A. (1999). Power laws in solar flares: Self-organized criticality or turbulence? *Physical Review Letters*, *83*, 4662–4665.

Boslough, M., Brown, P., & Harris, A. (2015). Updated population and risk assessment for airbursts from near-earth objects (NEOs). In *2015 IEEE aerospace conference* (pp. 1–12).

Bouchaud, J.-P., & Georges, A. (1990). Anomalous diffusion in disordered media: Statistical mechanisms, models and physical applications. *Physics Reports*, *195*, 127–293.

Brinkmann, R. (2013). *Florida sinkholes: Science and policy*: University Press of Florida.

Brown, P. G., Assink, J. D., Astiz, L., Blaauw, R., Boslough, M. B., Borovicvka, J., et al. (2013). A 500-kiloton airburst over Chelyabinsk and an enhanced hazard from small impactors. *Nature*, *503*, 238–241.

Brown, P., Spalding, R. E., ReVelle, D. O., Tagliaferri, E., & Worden, S. P. (2002). The flux of small near-Earth objects colliding with the Earth. *Nature*, *420*, 294–296.

Burridge, R., & Knopoff, L. (1967). Model and theoretical seismicity. *Bulletin of the Seismological Society of America*, *57*, 341–371.

Burroughs, S. M., & Tebbens, S. F. (2001). Upper-truncated power laws in natural systems. *Pure and Applied Geophysics*, *158*, 741–757.

Camacho, J., & Solé, R. V. (2001). Scaling in ecological size spectra. *Europhysics Letters*, *55*, 774–780.

Cannavò, F., & Nunnari, G. (2016). On a possible unified scaling law for volcanic eruption durations. *Scientific Reports*, *6*(1), 22289.

Casella, G., & Berger, R. L. (2002). *Statistical inference* (2nd ed.). Pacific Grove CA: Duxbury.

Cattuto, C., Loreto, V., & Pietronero, L. (2007). Semiotic dynamics and collaborative tagging. *Proceedings of the National Academy of Sciences of the United States of America*, *104*(5), 1461–1464.

Center for Near Earth Object Studies (2018). Fireball and Bolide Data: Jet Propulsion Laboratory. Retrieved from <https://cneos.jpl.nasa.gov/fireballs/>

Chavas, D. R., Lin, N., Dong, W., & Lin, Y. (2016). Observed tropical cyclone size revisited. *Journal of Climate*, *29*, 2923–2939.

Chialvo, D. R. (2010). Emergent complex neural dynamics. *Nature Physics*, *6*, 744–750.

Christensen, K., & Moloney, N. R. (2005). *Complexity and criticality*. London: Imperial College Press.

Clauset, A., Shalizi, C. R., & Newman, M. E. J. (2009). Power law distributions in empirical data. *SIAM Review*, *51*, 661–703.

Coles, S. (2001). *An introduction to statistical modeling of extreme values*. London: Springer.

Corominas-Murtra, B., Hanel, R., & Thurner, S. (2015). Understanding scaling through history-dependent processes with collapsing sample space. *Proceedings of the National Academy of Sciences of the United States of America*, *112*(17), 5348–5353.

Corral, A. (2004). Universal local versus unified global scaling laws in the statistics of seismicity. *Physica A*, *340*, 590–597.

Corral, A. (2006). Universal earthquake-occurrence jumps, correlations with time, and anomalous diffusion. *Physical Review Letters*, *97*, 178501.

Corral, A. (2008). Scaling and universality in the dynamics of seismic occurrence and beyond. In A. Carpinteri, & G. Lacidogna (Eds.), *Acoustic emission and critical phenomena* (pp. 225–244). London: Taylor and Francis.

Corral, A. (2009). Point-occurrence self-similarity in crackling-noise systems and in other complex systems. *Journal of Statistical Mechanics*, *P01022*.

Corral, A. (2010). Tropical cyclones as a critical phenomenon. In J. B. Elsner, R. E. Hodges, J. C. Malmstadt, & K. N. Scheitlin (Eds.), *Hurricanes and climate change* (Vol. 2, pp. 81–99). Heidelberg: Springer.

Corral, A. (2015). Scaling in the timing of extreme events. *Chaos, Solitons & Fractals*, *74*, 99–112.

Corral, A., Boleda, G., & Ferrer-i-Cancho, R. (2015). Zipf's law for word frequencies: Word forms versus lemmas in long texts. *PLoS ONE*, *10*(7), e0129031.

Corral, A., Deluca, A., & Ferrer-i-Cancho, R. (2012). A practical recipe to fit discrete power law distributions. *ArXiv*, *1209*, 1270.

Corral, A., Font, F., & Camacho, J. (2011). Non-characteristic half-lives in radioactive decay. *Physical Review E*, *83*, 66103.

- Corral, A., & Font-Clos, F. (2013). Criticality and self-organization in branching processes: Application to natural hazards. In M. Aschwanden (Ed.), *Self-organized criticality systems* (pp. 183–228). Berlin: Open Academic Press.
- Corral, A., Garcia-Millan, R., Moloney, N. R., & Font-Clos, F. (2018). Phase transition, scaling of moments, and order-parameter distributions in Brownian particles and branching processes with finite-size effects. *Physical Review E*, *97*, 062156.
- Corral, A., Ossó, A., & Llebot, J. E. (2010). Scaling of tropical-cyclone dissipation. *Nature Physics*, *6*, 693–696.
- Corral, A., Telesca, L., & Lasaponara, R. (2008). Scaling and correlations in the dynamics of forest-fire occurrence. *Physical Review E*, *77*, 16101.
- Corral, A., & Turiel, A. (2012). Variability of North Atlantic hurricanes: Seasonal versus individual-event features. In A. S. Sharma, A. Bunde, V. P. Dimri, & D. N. Baker (Eds.), *Extreme events and natural hazards: The complexity perspective* (pp. 111–125). Washington: Geopress.
- Cross, C. A. (1966). The size distribution of lunar craters. *Monthly Notices of the Royal Astronomical Society*, *134*, 245–252.
- Davidson, J., & Paczuski, M. (2005). Analysis of the spatial distribution between successive earthquakes. *Physical Review Letters*, *94*, 48501.
- del Castillo, J., Daoudi, J., & Serra, I. (2017). The full tails gamma distribution applied to model extreme values. *ASTIN Bulletin*, *47*, 895–917.
- del Castillo, J., & Puig, P. (1999). The best test of exponentiality against singly truncated normal alternatives. *Journal of the American Statistical Association*, *94*, 529–532.
- Deluca, A., & Corral, A. (2013). Fitting and goodness-of-fit test of non-truncated and truncated power law distributions. *Acta Geophysica*, *61*, 1351–1394.
- Dickman, R. (2003). Rain, power laws, and advection. *Physical Review Letters*, *90*, 108701.
- Ekström, G., Nettles, M., & Dziewoński, A. M. (2012). The global CMT project 2004–2010: Centroid-moment tensors for 13,017 earthquakes. *Physics of the Earth and Planetary Interiors*, *200–201*, 1–9.
- Emanuel, K. A. (1998). The power of a hurricane: An example of reckless driving on the information superhighway. *Weather*, *54*, 107–108.
- Emanuel, K. (2005a). *Divine wind: The history and science of hurricanes*. New York: Oxford University Press.
- Emanuel, K. (2005b). Increasing destructiveness of tropical cyclones over the past 30 years. *Nature*, *436*, 686–688.
- Farmer, J. D., & Geanakoplos, J. (2008). Power laws in economics and elsewhere. unpublished <http://tuvalu.santafe.edu/~jdf/papers/powerlaw3.pdf>
- Felzer, K. R., & Brodsky, E. E. (2006). Decay of aftershock density with distance indicates triggering by dynamic stress. *Nature*, *441*, 735–738.
- Ferrer-i-Cancho, R. (2016). Compression and the origins of Zipf's law for word frequencies. *Complexity*, *21*, 409–411.
- Florida Department of Environmental Protection (2004). Closed topographic depressions in Florida—2004 (*Tech. Rep.*): Florida Geological Survey. http://publicfiles.dep.state.fl.us/FGS/WEB/fava/fava_data/CTDS.zip
- Furusawa, C., & Kaneko, K. (2003). Zipf's law in gene expression. *Physical Review Letters*, *90*, 88102.
- Galve, J. P., Gutiérrez, F., Lucha, P., Guerrero, J., Bonachea, J., Remondo, J., & Cendrero, A. (2009). Probabilistic sinkhole hazard modelling. *Earth Surface Processes and Landforms*, *34*, 437–452.
- Galve, J. P., Remondo, J., & Gutiérrez, F. (2011). Improving sinkhole hazard models incorporating magnitude-frequency relationships and nearest neighbor analysis. *Geomorphology*, *134*(1), 157–170.
- Gaonac'h, H., Stix, J., & Lovejoy, S. (1996). Scaling effects on vesicle shape, size and heterogeneity of lavas from Mount Etna. *Journal of Volcanology and Geothermal Research*, *74*(1), 131–153.
- Gnedenko, B. V., & Korolev, V. Y. (1996). *Random summation: Limit theorems and applications*. Boca Raton: CRC Press.
- Godano, C., & Pingue, F. (2000). Is the seismic moment-frequency relation universal?. *Geophysical Journal International*, *142*, 193–198.
- Goldstein, M. L., Morris, S. A., & Yen, G. G. (2004). Problems with fitting to the power law distribution. *European Physical Journal B*, *41*, 255–258.
- Good, P. I. (2011). *Resampling methods* (3rd ed.). Boston: Birkhäuser.
- Gutenberg, B., & Richter, C. F. (1944). Frequency of earthquakes in California. *Bulletin of the Seismological Society of America*, *34*, 185–188.
- Gutiérrez, F., Fabregat, I., Roqué, C., Carbonel, D., Guerrero, J., García-Hermoso, F., et al. (2016). Sinkholes and caves related to evaporite dissolution in a stratigraphically and structurally complex setting, Fluvia Valley, eastern Spanish Pyrenees. Geological, geomorphological and environmental implications. *Geomorphology*, *267*, 76–97.
- Hanks, T. C., & Kanamori, H. (1979). A moment magnitude scale. *Journal of Geophysical Research*, *84 B*, 2348–2350.
- Hantson, S., Pueyo, S., & Chuvieco, E. (2016). Global fire size distribution: From power law to log-normal. *International Journal of Wildland Fire*, *25*, 403–412.
- Heimann, S., González, Á., Wang, R., Cesca, S., & Dahm, T. (2013). Seismic characterization of the Chelyabinsk meteor's terminal explosion. *Seismological Research Letters*, *84*(6), 1021–1025.
- Holme, P. (2019). Rare and everywhere: Perspectives on scale-free networks. *Nature Communications*, *10*, 1016.
- Ito, K., & Matsuzaki, M. (1990). Earthquakes as self-organized critical phenomena. *Journal of Geophysical Research*, *95*, 6853–6860.
- Johnson, N. L., Kotz, S., & Balakrishnan, N. (1994). *Continuous univariate distributions* (2nd ed., Vol. 1). New Jersey: Wiley-Interscience.
- Kagan, Y. Y. (1999). Universality of the seismic moment-frequency relation. *Pure and Applied Geophysics*, *155*, 537–573.
- Kagan, Y. Y. (2002). Seismic moment distribution revisited: I. Statistical results. *Geophysical Journal International*, *148*, 520–541.
- Kagan, Y. Y. (2010). Earthquake size distribution: Power law with exponent $\beta \equiv 1/2$? *Tectonophysics*, *490*, 103–114.
- Kagan, Y. Y. (2014). *Earthquakes: Models, statistics, testable forecasts*. West Sussex: Wiley.
- Kagan, Y. Y., Bird, P., & Jackson, D. D. (2010). Earthquake patterns in diverse tectonic zones of the globe. *Pure and Applied Geophysics*, *167*(6), 721–741.
- Kanamori, H., & Brodsky, E. E. (2004). The physics of earthquakes. *Reports on Progress in Physics*, *67*, 1429–1496.
- Knopoff, L., & Kagan, Y. (1977). Analysis of the theory of extremes as applied to earthquake problems. *Journal of Geophysical Research*, *82*, 5647–5657.
- Le Pichon, A., Ceranna, L., Pilger, C., Mialle, P., Brown, D., Herry, P., & Brachet, N. (2013). The 2013 Russian fireball largest ever detected by CTBTO infrasound sensors. *Geophysical Research Letters*, *40*, 3732–3737. <https://doi.org/10.1002/grl.50619>
- Li, W. (2002). Zipf's law everywhere. *Glottometrics*, *5*, 14–21.
- Limpert, E., Stahel, W. A., & Abbt, M. (2001). Log-normal Distributions across the Sciences: Keys and Clues. *BioScience*, *51*(5), 341–352.
- Lovejoy, S. (1981). Analysis of rain areas in terms of fractals. In *Proc. 20th Conference on Radar Meteorology*, American Meteorological Society (pp. 476–483).
- Lovejoy, S., & Mandelbrot, B. B. (1985). Fractal properties of rain, and a fractal model. *Tellus A*, *37A*(3), 209–232.
- Malamud, B. D. (2004). Tails of natural hazards. *Physics World*, *17*(8), 31–35.
- Malamud, B. D., Millington, J. D. A., & Perry, G. L. W. (2005). Characterizing wildfire regimes in the United States. *Proceedings of the National Academy of Sciences of the United States of America*, *102*, 4694–4699.
- Malamud, B. D., Morein, G., & Turcotte, D. L. (1998). Forest fires: An example of self-organized critical behavior. *Science*, *281*, 1840–1842.

- Malevergne, Y., Pisarenko, V., & Sornette, D. (2011). Testing the Pareto against the lognormal distributions with the uniformly most powerful unbiased test applied to the distribution of cities. *Physical Review E*, *83*, 36111.
- Mandelbrot, B. B. (1983). *The fractal geometry of nature*. New York: W. H. Freeman.
- Miller, G. A. (1957). Some effects of intermittent silence. *American Journal of Psychology*, *70*(2), 311–314.
- Minnich, R. A. (1983). Fire mosaics in Southern California and Northern Baja California. *Science*, *219*(4590), 1287–1294.
- Mitzenmacher, M. (2004). A brief history of generative models for power law and lognormal distributions. *Internet Mathematics*, *1*(2), 226–251.
- Moreno-Sánchez, I., Font-Clos, F., & Corral, A. (2016). Large-scale analysis of Zipf's law in English texts. *PLoS ONE*, *11*(1), e0147073.
- Moriña, D., Serra, I., Puig, P., & Corral, A. (2019). Probability estimation of a Carrington-like geomagnetic storm. *Scientific Reports*, *9*, 2393.
- Muñoz, M. A. (2018). Colloquium: Criticality and dynamical scaling in living systems. *Reviews of Modern Physics*, *90*, 31001.
- Navas-Portella, V., Serra, I., Corral, A., & Vives, E. (2018). Increasing power law range in avalanche amplitude and energy distributions. *Physical Review E*, *97*, 22134.
- Newman, M. E. J. (2005). Power laws, Pareto distributions and Zipf's law. *Contemporary Physics*, *46*, 323–351.
- Olami, Z., Feder, H. J. S., & Christensen, K. (1992). Self-organized criticality in a continuous, nonconservative cellular automaton modeling earthquakes. *Physical Review Letters*, *68*, 1244–1247.
- Pacheco, J. F., Scholz, C. H., & Sykes, L. R. (1992). Changes in frequency-size relationship from small to large earthquakes. *Nature*, *355*, 71–73.
- Pareto, V. (1897). *Cours d'économie politique, tome second*. Lausanne: F. Rouge, Libraire-Éditeur.
- Pawitan, Y. (2001). *In all likelihood: Statistical modelling and inference using likelihood*. Oxford: Oxford UP.
- Paylor, R. L., Florea, L., Caudill, M., & Currens, J. C. (2003). A GIS sinkhole coverage for the karst areas of Kentucky (Tech. Rep.): Kentucky Geological Survey. Retrieved from <http://www.uky.edu/KGS/gis/sinkpick.htm>
- Penland, C., & Sardeshmukh, P. D. (2012). Alternative interpretations of power law distributions found in nature. *Chaos: An Interdisciplinary Journal of Nonlinear Science*, *22*(2), 23119.
- Peters, O., & Christensen, K. (2002). Rain: Relaxations in the sky. *Physical Review E*, *66*, 36120.
- Peters, O., & Christensen, K. (2006). Rain viewed as relaxational events. *Journal of Hydrology*, *328*, 46–55.
- Peters, O., Christensen, K., & Neelin, J. D. (2012). Rainfall and dragon-kings. *The European Physical Journal Special Topics*, *205*(1), 147–158.
- Peters, O., Deluca, A., Corral, A., Neelin, J. D., & Holloway, C. E. (2010). Universality of rain event size distributions. *Journal of Statistical Mechanics*, P11030.
- Peters, O., Hertlein, C., & Christensen, K. (2002). A complexity view of rainfall. *Physical Review Letters*, *88*, 18701.
- Peters, O., & Neelin, J. D. (2006). Critical phenomena in atmospheric precipitation. *Nature Physics*, *2*, 393–396.
- Popova, O. P., & the Chelyabinsk Airburst Consortium (2013). Chelyabinsk airburst, damage assessment, meteorite recovery, and characterization. *Science*, *342*(6162), 1069–1073.
- Press, W. H., Teukolsky, S. A., Vetterling, W. T., & Flannery, B. P. (1992). *Numerical recipes in FORTRAN* (2nd ed.). Cambridge: Cambridge University Press.
- Pueyo, S., De Alencastro Graca, P. M. L., Barbosa, R. I., Cots, R., Cardona, E., & Fearnside, P. M. (2010). Testing for criticality in ecosystem dynamics: The case of Amazonian rainforest and savanna fire. *Ecology Letters*, *13*(7), 793–802.
- Pueyo, S., & Jovani, R. (2006). Comment on "A keystone mutualism drives pattern in a power function". *Science*, *313*, 1739c–1740c.
- Reed, W. J., & Hughes, B. D. (2002). From gene families and genera to incomes and internet file sizes: Why power laws are so common in nature. *Physical Review E*, *66*, 067103.
- Ross, S. M. (2010). *A first course in probability* (8th ed.). Englewood Cliffs: Prentice Hall.
- Rumpf, C. M., Lewis, H. G., & Atkinson, P. M. (2017). Asteroid impact effects and their immediate hazards for human populations. *Geophysical Research Letters*, *44*, 3433–3440. <https://doi.org/10.1002/2017GL073191>
- Saichev, A., Malevergne, Y., & Sornette, D. (2009). *Theory of Zipf's law and of general power law distributions with Gibrat's law of proportional growth*, Lecture Notes in Economics and Mathematical Systems. Berlin: Springer Verlag.
- Salje, E. K. H., Planes, A., & Vives, E. (2017). Analysis of crackling noise using the maximum-likelihood method: Power law mixing and exponential damping. *Physical Review E*, *96*, 42122.
- Sardeshmukh, P. D., Compo, G. P., & Penland, C. (2015). Need for caution in interpreting extreme weather statistics. *Journal Climate*, *28*(23), 9166–9187.
- Schorlemmer, D., & Wiemer, S. (2005). Microseismicity data forecast rupture area. *Nature*, *434*, 1086–1086.
- Schorlemmer, D., Wiemer, S., & Wyss, M. (2005). Variations in earthquake-size distribution across different stress regimes. *Nature*, *437*, 539–542.
- Schorlemmer, D., & Woessner, J. (2008). Probability of detecting an earthquake. *Bulletin of the Seismological Society of America*, *98*, 2103–2117.
- Serra, I., & Corral, A. (2017). Deviation from power law of the global seismic moment distribution. *Scientific Reports*, *7*, 40045.
- Serrà, J., Corral, A., Bogaña, M., Haro, M., & Arcos, J. Ll. (2012). Measuring the evolution of contemporary western popular music. *Scientific Reports*, *2*, 521.
- Shiryaev, A. N. (1996). *Probability* (2nd ed.). New York: Springer-Verlag.
- Simkin, M. V., & Roychowdhury, V. P. (2011). Re-inventing W. *Physics Reports*, *502*(1), 1–35.
- Simon, H. A. (1955). On a class of skew distribution functions. *Biometrika*, *42*, 425–440.
- Sornette, D. (2004). *Critical phenomena in natural sciences* (2nd ed.). Berlin: Springer.
- Sornette, A., & Sornette, D. (1989). Self-organized criticality and earthquakes. *Europhysics Letters*, *9*, 197–202.
- Taheri, K., Gutiérrez, F., Mohseni, H., Raeisi, E., & Taheri, M. (2015). Sinkhole susceptibility mapping using the analytical hierarchy process (AHP) and magnitude-frequency relationships: A case study in Hamadan province, Iran. *Geomorphology*, *234*, 64–79.
- Takayasu, H. (1989). *Fractals in the physical sciences*. Manchester: Manchester University Press.
- Traxl, D., Boers, N., Rheinwald, A., Goswami, B., & Kurths, J. (2016). The size distribution of spatiotemporal extreme rainfall clusters around the globe. *Geophysical Research Letters*, *43*, 9939–9947. <https://doi.org/10.1002/2016GL070692>
- Tria, F., Loreto, V., Servedio, V. D. P., & Strogatz, S. H. (2014). The dynamics of correlated novelties. *Scientific Reports*, *4*, 5890.
- Turcotte, D. L. (1997). *Fractals and chaos in geology and geophysics* (2nd ed.). Cambridge: Cambridge University Press.
- Utsu, T. (1999). Representation and analysis of earthquake size distribution: A historical review and some new approaches. *Pure and Applied Geophysics*, *155*, 509–535.
- Voitalov, I., van der Hoorn, P., van der Hofstad, R., & Krioukov, D. (2018). Scale-free networks well done. *arXiv*, 1811.02071.
- Wall, J., & Bohnenstiehl, D. R. (2014). Power-law relationship of sinkholes and depressions within karst geology. *Geological Society of America Abstracts with Programs*, *46*(3), 10.

- Wall, J., Bohnenstiehl, D. R., Wegmann, K. W., & Levine, N. S. (2017). Morphometric comparisons between automated and manual karst depression inventories in Apalachicola National Forest, Florida, and Mammoth Cave National Park, Kentucky, USA. *Natural Hazards*, *85*(2), 729–749.
- Wand, M. P. (1997). Data-based choice of histogram bin width. *The American Statistician*, *51*, 59–64.
- Wanliss, J. A., & Weygand, J. M. (2007). Power law burst lifetime distribution of the SYM-H index. *Geophysical Research Letters*, *34*, L04107. <https://doi.org/10.1029/2006GL028235>
- Watkins, N. W., Pruessner, G., Chapman, S. C., Crosby, N. B., & Jensen, H. J. (2016). 25 years of self-organized criticality: Concepts and controversies. *Space Science Reviews*, *198*, 3–44.
- White, E. P., Enquist, B. J., & Green, J. L. (2008). On estimating the exponent of power law frequency distributions. *Ecology*, *89*, 905–912.
- Woessner, J., & Wiemer, S. (2005). Assessing the quality of earthquake catalogues: Estimating the magnitude of completeness and its uncertainty. *Bulletin of the Seismological Society of America*, *95*(2), 684–698.
- Yang, W., Hauksson, E., & Shearer, P. M. (2012). Computing a large refined catalog of focal mechanisms for Southern California (1981–2010): Temporal stability of the style of faulting. *Bulletin of the Seismological Society of America*, *102*, 1179–1194.
- Yano, J.-I., Blender, R., Zhang, C., & Fraedrich, K. (2004). $1/f$ noise and pulse-like events in the tropical atmospheric surface variabilities. *Quarterly Journal of the Royal Meteorological Society*, *130*(600), 1697–1721.
- Yizhaq, H., Ish-Shalom, C., Raz, E., & Ashkenazy, Y. (2017). Scale-free distribution of Dead Sea sinkholes: Observations and modeling. *Geophysical Research Letters*, *44*, 4944–4952. <https://doi.org/10.1002/2017GL073655>
- Yoder, M. R., Holliday, J. R., Turcotte, D. L., & Rundle, J. B. (2012). A geometric frequency-magnitude scaling transition: Measuring $b = 1.5$ for large earthquakes. *Tectonophysics*, *532–535*, 167–174.
- Zanette, D. (2014). Statistical patterns in written language. *arXiv*, *1412.3336v1*.
- Zanette, D., & Montemurro, M. (2005). Dynamics of text generation with realistic Zipf's distribution. *Journal of Quantitative Linguistics*, *12*(1), 29–40.